ENGINEERING PROTEIN-BASED MATERIALS FOR NEOVASCULARIZATION

A Dissertation

by

GABRIELA GERALDO MENDES

Submitted to the Graduate and Professional School of
Texas A&M University
in partial fulfillment of the requirements for the degree of

DOCTOR OF PHILOSOPHY

Chair of Committee,	Sarah E. Bondos
Committee Members,	Kayla J. Bayless
	Carl A. Gregory
	Stephen H. Safe
Intercollegiate Faculty Chair,	David W. Threadgill

August 2021

Major Subject: Genetics

ABSTRACT

Protein-based materials have exceptional biological and mechanical properties, making these materials useful for many biomedical applications, including tissue engineering, drug delivery, enzyme immobilization, and biosensing. Bioactive materials can be created by genetically fusing a self-assembling protein to a functional protein. Key advantages of the protein fusion approach include elimination of a separate functionalization step during materials synthesis, uniform coverage of the material by the functional protein, and stabilization of the functional protein. The benefits of fusion protein materials offer opportunities to further develop this useful technique.

Previously, our lab has generated novel protein-based materials from the *Drosophila* Hox protein Ultrabithorax (Ubx), which self-assembles *in vitro*. Ubx materials are cytocompatible, biocompatible, biodegradable, and have tunable mechanical properties. Functionalization of Ubx materials can be accomplished via protein fusion, in which functional proteins are stabilized and retain their function while incorporated into materials. The unique properties of Ubx materials make them useful for a diverse range of applications.

In this work, we focused on developing Ubx-based materials to promote neovascularization. Stimulating neovascularization to support cell survival is critical for a variety of applications, including tissue engineering and wound healing.

Neovascularization is a multi-step, complex process that is promoted by several growth factors (GFs). Herein, we have genetically fused vascular endothelial growth factor (VEGF), stromal cell-derived factor 1α (SDF-1α), and basic fibroblast growth factor (bFGF) to Ubx in order to generate materials displaying pro-angiogenic GFs.

We confirmed that GFs remain active and stable when covalently incorporated into Ubx materials by the ability of fibers composed of GFs alone or in combination to induce endothelial cell (EC) migration and survival. We further demonstrated that Ubx materials displaying a combination of multiple GFs promote and guide neovascularization *in vivo* within 2 weeks in a mouse model. In addition, long-term studies suggested that GFs immobilized by Ubx materials induced vessel patency after 7 weeks.

Collectively, our data indicate that Ubx materials incorporating a combination of VEGF, bFGF, and SDF-1α promote the formation and stabilization of functional blood vessels. These materials have potential for use in tissue engineering and regenerative medicine, among other applications.

DEDICATION

I dedicate this dissertation to the 132 million girls who are out of school worldwide.

Eu dedico este trabalho às 132 milhões de meninas que estão fora da escola em todo o mundo.

ACKNOWLEDGEMENTS

I would like to thank my PhD advisor, Dr. Sarah Bondos, for being the best mentor that I could possibly have in Graduate School. I truly appreciate your support, kindness, and patience throughout this process. Words cannot express how grateful I am to have worked alongside you. I would also like to thank my committee members, Dr. Kayla Bayless, Dr. Carl Gregory, and Dr. Stephen Safe, for their guidance and helpful discussions throughout the course of this research.

Thanks go to former and current members of the Bondos lab, Dr. Rebecca Booth, Dr. David Howell, Dr. Shang-Pu Tsai, Dr. Kelly Churion, Sydney Tippelt, and Amanda Jons, for their help and assistance in the lab, but most importantly, for making my days and my experience much happier. I also thank all the undergraduates and high school students for the opportunity to train them. Thanks also go to the Bayless lab members, Colette Abbey, Timothy Sveeggen, and Ashley Coffell, for their technical help in the lab and for the funny moments we shared.

I would like to thank my colleagues, faculty, and staff from the Genetics Program and the Molecular and Cellular Medicine Department for all of the support and for making my time at Texas A&M University a great experience. I also thank Dr. Glassner and her lab members for their help with some of my experiments.

I will be forever grateful for my family for their unconditional love, support, and encouragement. My husband, Augusto, has been my best friend, always believing in me and helping me pursue my dreams. I thank him for his patience, for letting me vent my frustrations, and for being the most supportive and greatest partner for life. My parents, Solange and Americo, have always supported my decisions and encouraged me to achieve my goals. They have always made me feel safe and loved, and no matter how far they are always there for me. I thank them for letting me fly. My sister, Mariana, has been my best friend throughout my whole life and I share with her some of my favorite memories and moments. I thank her and my brother-in-law, Guilherme, for their support, affection, and love. My niece, Rafaela, and my nephew, Mateus, are the reason for my happiest smiles. Seeing my family on video calls in the past years has been the best part of my day and kept me motivated during Grad School.

I would also like to thank my friends from Brazil for their support and friendship. I especially thank Luciana and Taiuani for always encouraging me to pursue my PhD in the US and being present in my life. I also thank my friends Livia and Davi for being our family away from home and giving us our nephews Benjamin and Pete. Thanks also go to Vera, Aladimar, Pedro, and Alice for being my second family, always supportive and loving. Finally, I thank my psychologist Larissa for helping me to learn more about myself, deal with my anxiety, and take care of my mental health.

CONTRIBUTORS AND FUNDING SOURCES

Contributors

This work was supervised by a dissertation committee consisting of Professors Sarah E. Bondos, Kayla J. Bayless, and Carl A. Gregory of the Department of Molecular and Cellular Medicine and Professor Stephen H. Safe of the Department of Department of Veterinary Physiology and Pharmacology.

The data presented in Chapter 2 was collected in part by former postdoctoral researcher, Dr. David Howell, who performed the *in vitro* assays and long-term implantations in mice, while analyses of the results were performed by the student. The 2-week mice data was collected and analyzed by the student.

All other work conducted for the dissertation was completed by the student independently.

Funding Sources

Graduate study was supported by a fellowship from the Brazilian National Council for Scientific and Technological Development (CNPq). This work was also made possible in part by the National Institutes of Health (NIH), under grant number R41GM134776-01. Its contents are solely the responsibility of the authors and do not necessarily represent the official views of these institutions.

TABLE OF CONTENTS

Page

LIST OF FIGURES

Page

LIST OF TABLES

Page

CHAPTER I

GENERAL INTRODUCTION AND LITERATURE REVIEW*

1.1 Protein-based materials and their unique properties and advantages

Proteins can reversibly bind specific molecules with high affinity by forming multiple weak bonds with ligands. *In vivo*, proteins require these traits to create and regulate the vital molecules, cells, and tissues necessary for all life. The wide variety of natural protein functions has been further augmented by engineering proteins with novel abilities (Glasscock et al., 2016; Vornholt & Jeschek, 2020). Embedding active proteins in materials imparts these efficient and specific functions to devices that can be engineered for many applications, including biomolecular sensors (Horak et al., 2018; Hu et al., 2019; Wei et al., 2017), drug delivery (Petrou et al., 2018; Wolinsky et al., 2012), chemical catalysis (Dean et al., 2017), and tissue engineering (Goor et al., 2017; Hollingshead et al., 2017; Seliktar, 2012; Wei et al., 2017; Wang et al., 2008).

Protein-based materials have many advantages. This platform provides a facile method to embed and stabilize proteins with useful functions into the materials, and the fidelity of transcription and translation (1 error per 10^4 amino acids) ensures that each protein unit is consistent in length and amino acid sequence (Abbas et al., 2017; Cochella & Green, 2005; Girotti et al., 2015; Wang et al., 2015). Thus, proteins produced from a single gene in a constant environment will have the same three-dimensional structure and stability, and, for proteins that

*Part of Chapter 1 is reprinted with permission from "Generating novel materials using the intrinsically disordered protein Ubx" by Mendes GG, Booth RM, Pattison DL, Alvarez AJ, and Bondos SE, 2018. Methods in Enzymology, 611, 583-605, Copyright 2018 by Elsevier Inc.

form higher-order complexes, the same ability to assemble (Abbas et al., 2017; Girotti et al., 2015). Protein-based biomaterials can have useful mechanical properties, including extreme strength, as exemplified by dragline silk, and high extensibility, as observed for elastin and elastin-like proteins (ELPs). Finally, the sequence of the protein monomers can be easily and quickly engineered using standard molecular biology techniques, allowing the materials' sequence, assembly mechanism, structure, stability, and physical properties to be tailored for specific applications (Kim et al., 2014).

As a normal component of the body, proteins are generally biodegradable (Girotti et al., 2015; Kowalczyk et al., 2014; NHCS Silva et al., 2014; R Silva et al., 2014; Unzueta et al., 2017) and non-toxic (Romano et al., 2011), with some exceptions such as toxins from snake venom or harmful bacteria. Although protein monomers can elicit antibody production when injected into an animal host, assembly of these monomers into a stable material tends to prevent an immune response (Park et al., 2010; Patterson et al., 2015; Y Wang et al., 2008; Zhou et al., 2010). Indeed, many recombinant materials-forming proteins produced in bacteria or insects are biocompatible and non-immunogenic (Girotti et al., 2015; Patterson et al., 2014; Patterson et al., 2015). Consequently, protein-based materials are often also biocompatible and thus suitable for *in vivo* applications (Agnieray et al., 2021; Girotti et al., 2015; Kowalczyk et al., 2014; NHCS Silva et al., 2014; R Silva et al., 2014; Unzueta et al., 2017).

Because the three-dimensional native structure of proteins is primarily stabilized by non-covalent bonds, the structure of protein monomers, and in some cases protein assemblies, can respond to changes in environmental conditions (Solomonov & Shimanovich, 2019). These

properties can not only diversify the form of materials produced from a single protein, but also create smart materials that alter form and function in response to specific cues (Parker et al., 2020).

1.2 Biomaterials composed of naturally derived self-assembling proteins

A subset of proteins naturally self-assembles into useful biomaterials. Several prominent examples include silk, elastin, collagen, and resilin (Agnieray et al., 2021; Balu et al., 2021; Hu et al., 2012). Silk proteins are naturally synthesized by spiders and silkworms, such as N. clavipes and B. mori, respectively (NHCS Silva et al., 2014; Dinjaski et al., 2017; Hu et al., 2012). Natural silks have a long history of use in medicine, applied as surgical sutures, for example (Mackenzie, 1973; Muffly et al., 2011). These proteins are challenging to produce as recombinant monomers and to assemble into materials *in vitro*; therefore, many labs have developed modified versions of these proteins to ameliorate these problems. These modified proteins are often still referred to as the natural protein (e.g., "silk") despite deletions, additions, and/or alterations to the protein sequence. The biocompatibility and mechanical properties of silks have made them valuable tools for many applications (Jansson et al., 2014), including bone regeneration (Dinjaski et al., 2017; Plowright et al., 2016), soft tissue regeneration (Bellas et al., 2015), cell adhesion (Pereira et al., 2017), cardiac tissue engineering (Petzold et al., 2017), and drug delivery (Doblhofer & Scheibel, 2015).

As components of the extracellular matrix, collagen and elastin have chemical and mechanical properties capable of supporting cell growth to create extensible or flexible tissues (NHCS Silva et al., 2014; Yeo et al., 2015). Collagen-based materials have been created for

tissue engineering (Copes et al., 2019; Gomes et al., 2012), wound healing (Cao et al., 2020; Deshmukh et al., 2016), and drug and gene delivery (Grønlien et al., 2019; Urello et al., 2014). These applications are made possible by collagen's biocompatibility, weak antigenicity, and biodegradability (Copes et al., 2019). As proteins that have evolved to support and interact with cells, materials composed of elastin-like recombinamer (ELR) are being developed for applications in skin tissue engineering and wound healing (Da Costa et al., 2017), among others.

Resilin is an elastomeric protein found in insect cuticles, which is characterized by low stiffness and high energy storage capacity, making them elastic, extensible, and resilient (Girotti et al., 2015; Hu et al.; 2012; Li et al., 2016). Resilin has important roles for flight in arthropods, leg movement in arachnids, vocalization in cicadas, and jumping in fleas (Girotti et al., 2015; Lyons et al., 2009). Resilin's mechanical and biological properties make it a very promising scaffold for strong but flexible tissues such as vocal cords (Li et al., 2011; Li et al., 2016) and blood vessels (Y Kim et al., 2016; McGann et al., 2013). Moreover, extensible and conductive hydrogels based on recombinant resilin have been developed for application as wearable sensors (Hu et al., 2019).

In addition, hybrid fusion proteins have also been created to combine the properties of silk, collagen, elastin, resilin, and/or cartilage oligomeric matrix proteins (Grieshaber et al., 2009; Grieshaber et al., 2012; Isaacson et al., 2018; Krishna et al., 2011; Pereira et al., 2017; Yuvienco et al., 2012). Because the protein domains that determine the mechanical properties are modular, different combinations of these protein sequences can be created to optimize the mechanical properties of the hybrid material for a specific application (Bax et al., 2019;

Bracalello et al., 2011; Huang et al., 2015; Qiu et al., 2009; Wang et al., 2018; Włodarczyk-Biegun et al., 2014).

1.3 Ultrabithorax (Ubx) materials

Occasionally, a protein that does not form materials as part of its native function is able to self-assemble *in vitro*. This is the case for a novel biomaterial discovered by our lab. The *Drosophila melanogaster* Hox transcription factor Ultrabithorax (Ubx) is capable of materials formation *in vitro*. The unique properties and applications of these materials are the focus of this dissertation.

During animal development, Ubx binds DNA to activate or repress the transcription of target genes. Although capable of cooperative DNA binding (Beachy et al., 1993), Ubx does not form materials as part of its natural function. Despite the lack of evolutionary selection for self-assembly, Ubx monomers hierarchically form ordered materials on a variety of length scales *in vitro* (Figure 1). In buffers near neutral pH, Ubx coacervates at the air–water interface, generating disorganized clusters (aggregates) of molecules (Greer et al., 2009; Majithia et al., 2011). These clusters reshape themselves into lines, or protofibrils. Lateral interactions between protofibrils condense them into fibrils, which are similar in diameter to amyloid fibrils but lack amyloid structure. Fibrils interact laterally to form film, and film can be drawn into fibers that are meters long, with diameters ranging from 2 to 100 μm, depending on the thickness of the film.

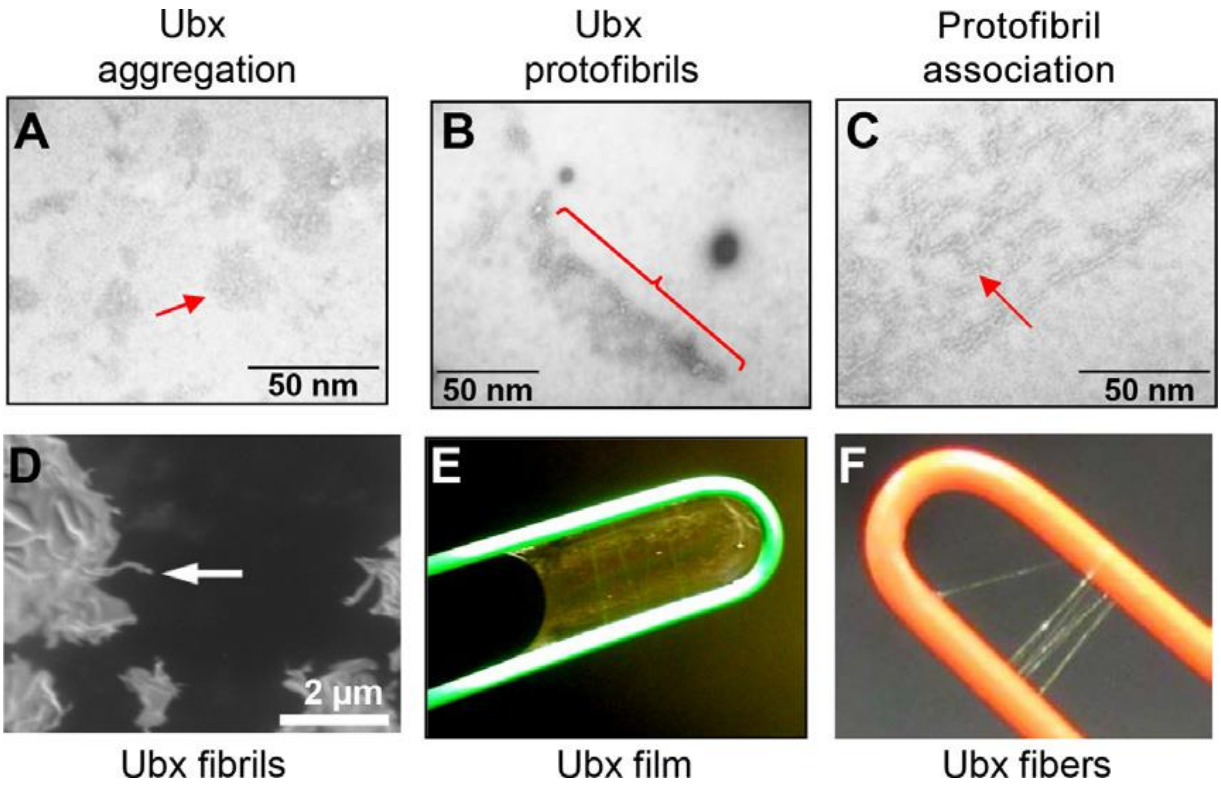

Figure 1. Ubx self-assembles into materials in vitro.
(A) About 15 min after dilution into a tray, Ubx begins to form irregular aggregates (red arrow). (B) Within 1h, these aggregates begin to spontaneously reshape into lines of Ubx proteins, termed protofibrils. (C) After 1–2 h, the protofibrils align in parallel and begin to form side-to-side contacts. (D) After 2h multiple protofibrils condense to form fibrils about 50nm in diameter (white arrow). (E) Fibrils also interact laterally to form films which can be lifted from the surface. (F) Alternately, films on the air–water interface can be drawn into fibers composed of aligned fibrils. Figure reprinted with permission from Mendes GG, Booth RM, Pattison DL, Alvarez AJ, and Bondos SE. Generating novel materials using the intrinsically disordered protein Ubx 2018. Methods in Enzymology, 611, 583-605, Copyright 2018 by Elsevier Inc.

The strength of Ubx materials is derived from the rapid and spontaneous formation of dityrosine bonds, and mutation of tyrosine residues can either weaken or strengthen the resulting materials (Howell et al., 2015; Huang et al., 2010). Furthermore, Ubx materials have tunable mechanical properties (Greer et al., 2009; Howell et al., 2015; Huang et al., 2010) and are

cytocompatible (Patterson et al., 2014), biocompatible and non-immunogenic (Patterson et al., 2015), and biodegradable (Hsiao et al., 2016). These unique properties are advantageous and needed for a variety of biomedical applications.

1.4 Functionalization of protein-based materials

1.4.1 Incorporation of proteins into materials via protein fusion

Protein-based materials offer a unique opportunity to efficiently immobilize and display useful functional proteins. Simple molecular biology tools can be used to produce both functional and self-assembling proteins as a single linear amino acid chain linked by a covalent peptide bond (Girotti et al., 2015; Huang et al., 2011; Jansson et al., 2014) (Figure 2). The sequence of amino acids is unique to each protein and genetically encoded by the sequence of nucleic acids in that protein's gene (DNA), which is also a linear sequence. To create a "fusion gene", the DNA sequence encoding the functional protein is placed end-to-end with the DNA sequence encoding the self-assembling protein, without intervening stop codons. When the appropriate regulatory DNA sequences are added to the fusion gene and it is placed in a live cell (Figure 2, Step 1), the cell will use the DNA instructions to produce a single "fusion protein" that contains the amino acid sequence of both proteins in a single chain of amino acids (Figure 2, Step 2). In the example shown in Figure 2, the functional protein sequence is followed by the sequence of the self-assembling protein. Ideally, these proteins will independently fold into their unique 3-dimensional structures as defined by their amino acid sequence (Figure 2, Step 3), and the self-assembling portion of the fusion protein will interact with other copies of the fusion protein to form materials. In practice, an additional short linker sequence of amino acids must be

added in between the functional sequence and the self-assembling sequence to prevent one sequence from sterically hindering the folding or function of the adjacent sequence.

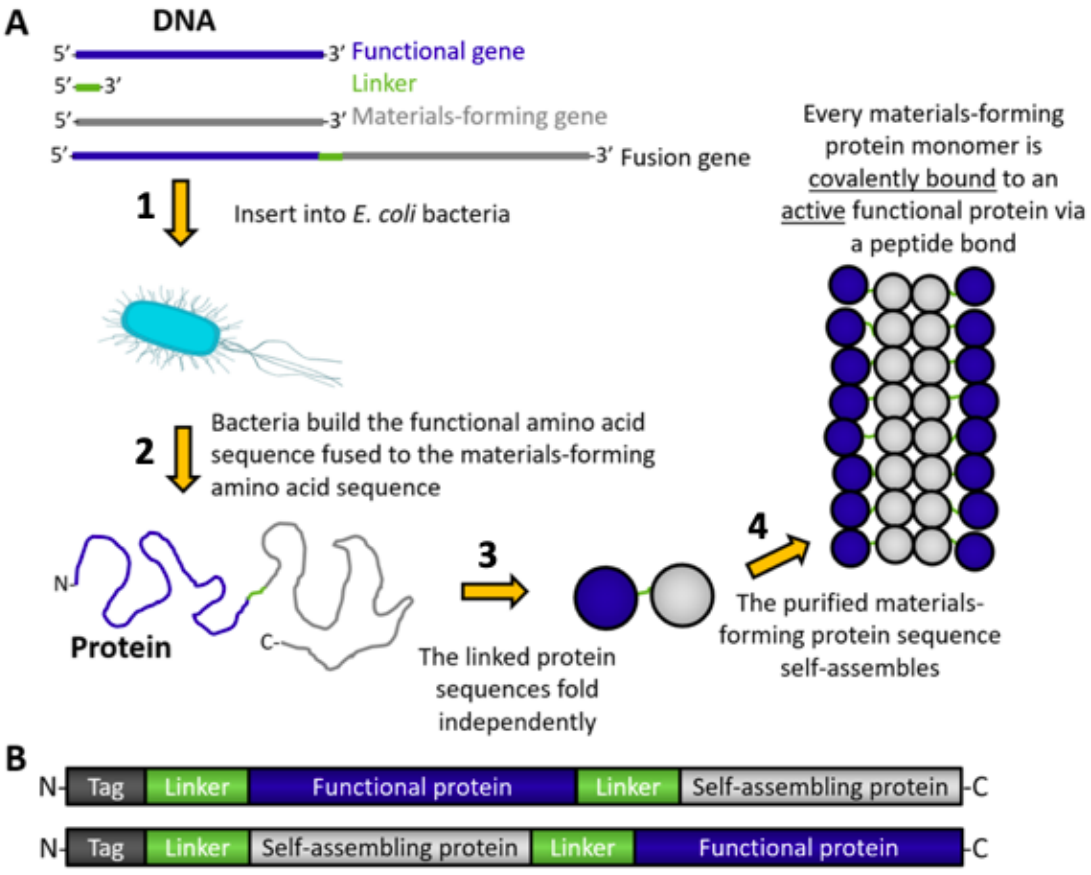

Figure 2. Fusion proteins in materials assembly.
(A) A schematic depicting the production of fusion proteins and their assembly into materials. (B) Schematic of fusion protein sequences. The functional protein (dark blue) may be placed N-terminal (top) or C-terminal (bottom) to the self-assembling protein (grey) or within a flexible loop of the self-assembling protein. Purification tags (dark grey) may be included at either terminus or within the protein sequence. Soluble, flexible linkers (green) are often required to prevent each component from sterically interfering with the folding or function of other components within the fusion protein.

1.4.2 Protein fusion and its advantages

There are numerous advantages to the protein fusion approach. By combining production of the functional protein, production of the self-assembling protein, and protein immobilization into a single-step, one-pot process, the time and cost required to produce materials is substantially reduced (Gomes et al., 2011; Zhou et al., 2014). Furthermore, the extent of functionalization does not need to be independently validated after each production batch. The added functional protein has the potential to increase the yield of the recombinant fusion protein, an effect that has been observed in *E. coli* (Pereira et al., 2017; Tsai et al., 2015) and in the silkworm *Bombyx mori* (Inoue et al., 2005). This increase in yield correlates with the solubility of the fusion protein (Tsai et al., 2015) and can help prevent the random (non-productive) association of monomers into aggregates (Park et al., 2007).

The functional proteins are uniformly attached to the material by the same bond. Consequently, there are no variations in the attachment site, which may have the potential to misposition or inactivate a portion of the functional protein. Because the functional protein is attached to the material via a peptide bond, any solution conditions that are safe for the materials will also preserve this bond, reducing or eliminating leaching (Brady & Jordaan, 2009). Every monomer has one functional protein attached; thus, by definition, the materials are saturated, and the coverage is even.

Many proteins fused to protein materials exhibit increased stability relative to their soluble monomers (Jansson et al., 2015; Tsai et al., 2015), although this is not the case for all fusion proteins that form materials (Wang et al., 2018). Finally, many different proteins can be

incorporated and even patterned within a single material as protein fusions (Huang et al., 2011). In many cases, the addition of a functional protein does not harm either monomer production or materials assembly (Jansson et al., 2014; Jansson et al., 2015; Thatikonda et al., 2016; Tsai et al., 2015).

The functionality of the appended functional protein is often preserved in protein materials. Incorporating functional proteins into materials can stabilize these proteins relative to the corresponding free protein monomer. The fluorescence intensity of mCherry is retained in mCherry-Ubx fibers even after ethanol treatment for 30 minutes (80%) or autoclaving for 20 minutes (20%), a trait that facilitates materials sterilization (Tsai et al., 2015). This increase in stability can assist with materials storage as well. The enzyme xylanase was 40% active after 11 months of wet storage, >1 month of dry storage, or 70% ethanol treatment when incorporated into materials formed by an engineered spider silk protein (Jansson et al., 2015). The source of this incredible stability is likely due to the confined geometry effect, in which functional proteins embedded within the materials lack the space required for the large-scale motions associated with protein unfolding (Frauenfelder et al., 2006; Mittal & Best, 2008; Rathore et al., 2006).

Finally, more than two genes may be fused, thus incorporating multiple proteins and functions into the same polypeptide. One example of a multi-fusion protein is resilin–elastin–collagen chimeric recombinant materials, designed to tailor the mechanical properties of the resulting materials (Bracalello et al., 2011).

1.4.3 Protein fusion challenges

While many proteins have been successfully incorporated into materials via protein fusion, several steps may pose challenges. For functional proteins with properties that impede materials assembly, one option is to select a related protein that retains the same function yet has better properties for assembly. For example, ancestral proteins or proteins from thermophiles may be more compact and/or more stable (Sawle & Ghosh, 2011). Another option is to mutate the protein to stabilize the protein (Borgo & Havranek, 2012) or alter the surface chemistry. However, because a single amino acid change may simultaneously impact protein structure, solubility, and/or function, this process can unintentionally harm protein function as well. Because the goal of creating the materials is often to incorporate a very specific protein, it is often not feasible to replace or mutate the functional protein.

Many protein-based materials are assembled in harsh conditions (e.g., high temperature, low pH, or organic solvents), which are likely to unfold or inactivate most functional proteins (Falconnet et al., 2006; Hahn et al., 2005; Huang et al., 2011; Tsai et al., 2015) (Figure 3). The most feasible solution to this problem is to, when possible, assemble materials in near physiological conditions to maintain the activity of the appended protein (Huang et al., 2011; Jansson et al., 2014). In some cases, the sequence of the self-assembling protein can be engineered to allow assembly in conditions that preserve the activity of the fused protein (Jansson et al., 2014).

Several other considerations can complicate materials generation. Materials assembly, even in physiological conditions, can theoretically denature or inactivate the functional protein

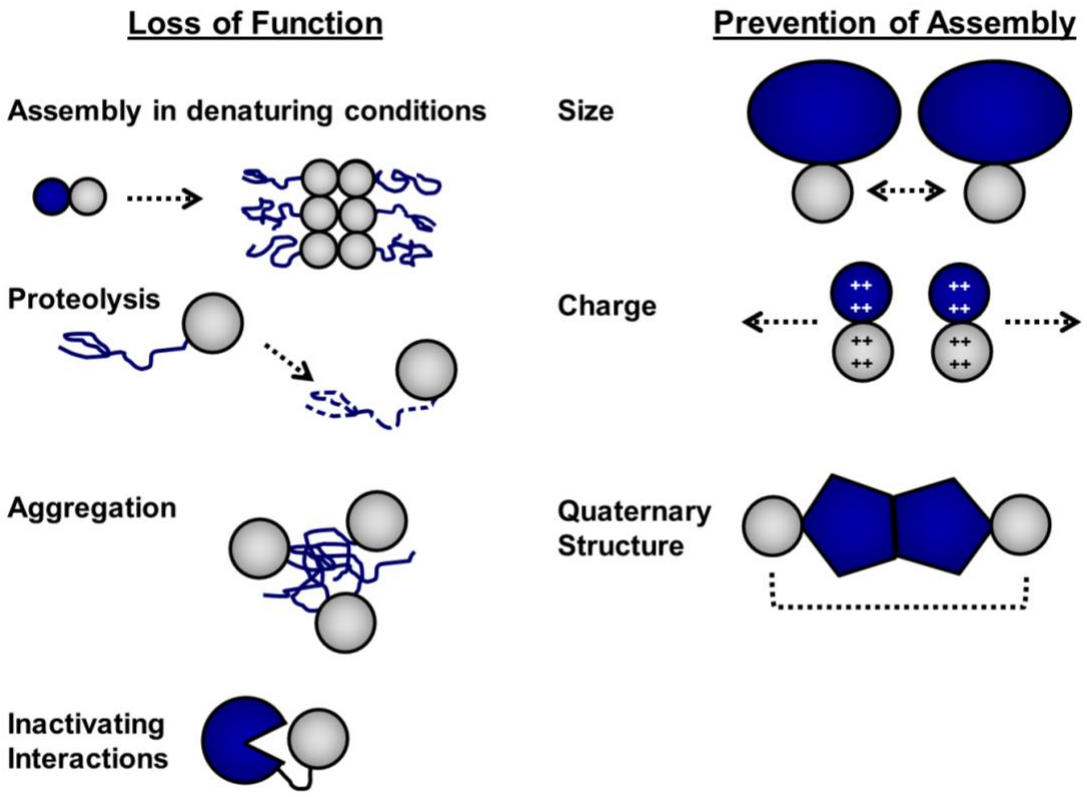

Figure 3. Potential problems caused by fusion proteins fall into two main categories, Loss of Function and Prevention of Assembly.
Loss of function can be caused by the self-assembling protein (grey) inactivating the functional protein (dark blue), which in turn can lead to proteolysis or aggregation. In addition, direct binding by the functional protein to the self-assembling protein could sequester critical protein surfaces needed for either function or materials assembly. Furthermore, the functional protein could prevent contact between self-assembling proteins because they are too large, too charged, or because quaternary structure mis-positions the self-assembling protein monomers.

(Zhou et al., 2014) (Figure 3). If folding of the functional protein yields less free energy than assembly of the materials, then assembly could drive denaturation of the functional protein. The materials-forming protein may form additional, non-covalent interactions with the functional

protein that inactivate the functional component (e.g., physically block a ligand binding site), in both the monomeric and assembled states.

The reverse problem can also occur, in which the functional protein impairs or prevents materials assembly. Highly charged functional proteins may slow or prevent materials assembly through charge-charge repulsion. Furthermore, functional proteins with quaternary structure (e.g., dimers, trimers) have the potential to mis-position the self-assembling protein and prevent materials assembly (Tsai et al., 2015) (Figure 3).

1.5 Functionalization of Ubx materials

The large intrinsically disordered regions within the Ubx sequence enable the successful incorporation of a wide variety of proteins into materials, including fusions to proteins nearly ten times the size of Ubx, to highly charged proteins, or to dimers/tetramers without impacting its ability to form materials (Tsai et al., 2015).

We see evidence for this when we compare Ubx monomer assembly with Enhanced Green Fluorescent Protein-Ubx (EGFP-Ubx) monomer assembly. If EGFP impaired Ubx assembly, then the fraction of Ubx protein in the material should be higher than the fraction of Ubx in the monomer mixture. Instead, the ratio of Ubx and EGFP-Ubx proteins in the final material was the same as in the initial protein mixture. Therefore, both proteins assemble equally well (Tsai et al., 2015). Furthermore, the addition of EGFP to VEGF-Ubx improved the solubility, and thus monomer yield during production in *E. coli*. (Howell et al., 2016). The

EGFP-VEGF-Ubx double fusion also self-assembled into materials, which retained both green fluorescence and VEGF activity (Howell et al., 2016).

Because of its robust assembly and incorporation of functional proteins, Ubx is a useful platform for generating active biomaterials. Furthermore, sequence similarities between Ubx and other self-assembling proteins suggest that this approach for generating fibers and film in aqueous conditions near neutral pH might be successfully applied to other protein systems.

1.6 Applications of protein-based materials

Protein materials can be easily optimized for many applications (Cai & Heilshorn, 2014; Romano et al., 2011). Opportunities for specific applications arise both from the general properties of each protein material and the range of proteins that can be incorporated as protein fusions. This modular approach allows the inclusion of one or more functional peptides or proteins into a single protein sequence with tunable properties (Cai & Heilshorn, 2014; Tsai et al., 2015). Protein-based materials are being developed for a variety of biomedical and biotechnological applications such as chemical catalysis, antibody capture and immobilization, cell binding, tissue engineering and regenerative medicine, and drug delivery (Balu et al., 2021; Dean et al., 2017; Goor et al., 2017; Hollingshead et al., 2017; Horak et al., 2018; Howell et al., 2016; Petro et al., 2018; Seliktar, 2012; Z Wang et al., 2008; Wei et al., 2017; Wolinsky et al., 2012).

The efficiency, stereoselectivity, and catalytic activity of enzymes in environmentally friendly conditions have increased the interest in using enzymes for industrial chemical

production (Jansson et al., 2015; Jia et al., 2014). Chemical catalysis through the immobilization and stabilization of enzymes on solid supports has many advantages, including facile separation of enzymes from the reaction mixture, which both allows enzyme recovery and aids product purification (Zhou et al., 2014). Additionally, these advantages reduce product cost, which is an especially important aspect in industrial processes (Jansson et al., 2015). Although most immobilization strategies have relied on either physical entrapment, biotin/streptavidin recognition, adsorption, or nonspecific binding to a flat or microparticle surface (Jia et al., 2014), enzymes have also been genetically fused to materials-forming proteins, including the silk derivative 4RepCT, Ubx, and the amyloidogenic protein Ure2, and retained their activity once inside these materials (Huang et al., 2011; Jansson et al., 2015; Tsai et al., 2015). One key challenge in multi-step enzyme-mediated chemical catalysis is the need to place multiple enzymes in close proximity to limit product diffusion (Jia et al., 2014). Nature sometimes solves this problem by fusing together multiple enzymes that catalyze different steps in a series of chemical reactions (Maier et al., 2008; Zhu & Xiong, 2013). Materials composed of fusion proteins provide a unique opportunity to manipulate the geometry of enzyme packing to reduce product diffusion within the materials, and thus increase reaction yields.

Many protein-based materials applications are based on the functionalization of materials with affinity domains that recognize antibodies. Once antibodies non-covalently bind these materials, the materials can be potentially used to bind specific ligands (as in sensors) (Kim et al., 2011), bind and display proteins (for tissue engineering applications) (Jansson et al., 2014), or deliver proteins (for therapeutics) (Jansson et al., 2014; Thatikonda et al., 2016). In this versatile approach, the same base material can be used with any antibody/antigen combination.

In particular, effective immobilization of antibodies on a solid support is of extreme importance for the specificity and sensitivity of immunoassay procedures (Kim et al., 2011; Vashist et al., 2014).

Many materials have been modified via peptide fusion to improve binding to specific types of cells. Integrin- and fibronectin-binding sequences were inserted into the collagen-like protein Scl2 from *Streptococcus pyogenes* fused to recombinant silk, creating chimeric collagen-silk fibers, allowing these materials to attach and grow human mesenchymal stem cells (hMSCs) (An et al., 2013). The great variety of peptides that recognize specific types of normal vs. diseased cells (Gray & Brown, 2014) have the potential to increase cell attachment and migration to materials for applications involving diverse tissues (Widhe et al., 2016). These tools make peptide fusion materials a particularly powerful tool for cell analysis (cell isolation, detection) and tissue engineering (cell attachment and patterning) applications.

Protein-based materials are widely applied in tissue engineering and regenerative medicine (Agnieray et al., 2021; Dinjaski et al., 2017; Girotti et al., 2015; Gomes et al., 2011; Gomes et al., 2012; Pereira et al., 2017). Because cells respond to both mechanical and chemical cues, matching the materials' properties to the target tissue is very important for tissue regeneration or engineering. The sequence of recombinant self-assembling proteins can be easily modified to alter the structural or mechanical properties of the resulting materials using standard molecular biology techniques, as in hybrid materials composed of silk elastin and collagen sequences (Bax et al., 2019; Grieshaber et al., 2009; Grieshaber et al., 2012; Huang et al., 2015; Isaacson et al., 2018; Krishna et al., 2011; Pereira et al., 2017; Qiu et al., 2009; Wang et al.,

2018; Włodarczyk-Biegun et al., 2014). This plasticity allows the properties of the materials to be tailored to suit a variety of applications (Dinjaski et al., 2017; Unzueta el al., 2017). A large number of proteins and peptides function as chemical cues that control cell behavior and support cell growth, attachment, and proliferation within the scaffold. In addition to peptides, growth factors (generally dimeric proteins) have also been fused to materials to direct cell behavior.

Protein-based materials also have the potential to be used as drug delivery systems (Agnieray et al., 2021; Kowalczyk et al., 2014; NHCS Silva et al., 2014). Genetically engineered biomaterials that are biocompatible, biodegradable, and bind ligands with high specificity have the potential to be used for the controlled release of drugs and other molecules (Huang et al., 2015; Petrou et al., 2018; Pritchard & Kaplan, 2011). Recombinant lipid-ELP biomaterials have been developed to self-assemble into drug delivery micelles of different sizes and shapes that can encapsulate hydrophobic anti-cancer drugs, such as doxorubicin and paclitaxel (Luginbuhl et al., 2017).

1.7 Application of protein-based materials for scaffold neovascularization

Stimulating neovascularization or formation of new blood vessels is needed for many critical applications. As an example, in tissue engineering and regenerative medicine fields, the adequate perfusion of larger size scaffolds (Chandra & Atala, 2019; Mastrullo et al., 2020; Yang et al., 2020) and the integration of the vascular network from engineered tissues to the patient's vasculature are necessary for the nourishment and regeneration of the bioengineered constructs (Ngo & Harley, 2020; Rouwkema & Khademhosseini, 2016; Yao et al., 2020). Blood vessels are also essential for wound healing, especially in the treatment of chronic wounds, such as diabetic

foot ulcers, in which poor vascularization correlates to impaired wound healing (Atienza-Roca et al., 2018; Demidova-Rice et al., 2012; Jahani et al., 2020; Niu et al., 2019; Zubair & Ahmad, 2019).

Neovascularization occurs either by vasculogenesis or by angiogenesis (Ucuzian et al., 2010). Because vasculogenesis occurs at the embryo development level, here we will focus on angiogenesis, which is defined as the formation of new vessels by the growth and sprouting of preexisting vessels (Carmeliet, 2000; Carmeliet & Jain, 2011; Herbert & Stainier, 2011; Lamalice et al., 2007). This process requires spatiotemporal delivery of bioactive molecules, especially growth factors (GFs) and chemokines, to create a stable and functional vascular network (Cao & Mooney, 2007; Kant & Coulombe, 2018; Mastrullo et al., 2020).

1.8 Delivery of growth factors to stimulate neovascularization

Growth factors can induce neovascularization by stimulating endothelial cells (ECs) migration, proliferation, and recruiting mural cells (pericytes and smooth muscle cells) to form and stabilize new blood vessels (Carmeliet, 2000; Carmeliet & Jain, 2011). Consequently, most engineering studies have focused on GFs to stimulate angiogenesis (Cao & Mooney, 2007; Chandra & Atala, 2019; Gianni-Barrera et al., 2019; Mastrullo et al., 2020; Nazeer et al., 2021). However, there are several challenges in delivering GFs. Natural GFs have short effective half-life, mainly because of poor stability in physiological environment (Baiguera & Ribatti, 2013; Mitchell et al., 2016; Niu et al., 2019; Ren et al., 2020), fast blood clearance (Mitchell et al., 2016), and/or rapid degradation by enzymes (Ren et al., 2020; Wang et al., 2017). GFs as

recombinant proteins also present poor stability *in vivo* (Niu et al., 2019), being rapidly degraded or deactivated prior to reaching their target (Masters, 2011).

The concentration of delivered GFs needs to be precise, thus safety is another concern (Niu et al., 2019). Because of low stability and short half-life, GFs often need to be administered multiple times or using supraphysiological doses to maintain the necessary concentration at the delivered site, which results in higher cost (Niu et al., 2019; Ren et al., 2020) and adverse side effects (Baiguera & Ribatti, 2013; Ren et al., 2020). GFs are also involved in cancer progression (Witsch et al., 2010) and the repeated administration of supraphysiological doses increases the risk of developing cancer (Niu et al., 2019). Examples of GFs approved for clinical use include Regranex® gel, composed of recombinant human PDGF-BB, used to treat diabetic foot ulcers, and AMPLIFY™, based on recombinant human bone morphogenetic protein-2 (BMP-2), used in lumbar spinal arthrodesis, and both have been associated with an increased risk of new cancer (Niu et al., 2019; FDA 2008; Carragee et al., 2013). Another limitation of GFs delivery is the maintenance of GF activity in materials over weeks to create mature blood vessels. For instance, it has been shown that newly formed vessels induced by VEGF *in vivo* completely disappears after a limited VEGF exposure. However, VEGF simulation maintained for 10 to 14 days results in the formation of mature vasculature that does not regress after withdrawal of the GF (Dor et al., 2002).

1.9 Biomaterials as strategies to deliver growth factors

Incorporation of GFs into biomaterials has the potential to overcome the limitations of soluble GF delivery (Atienza-Roca et al., 2018; Wang et al., 2017). Immobilization of GFs into

biomaterials can achieve controlled, sustained release and localized delivery, as well as reduce the need for multiple doses and, thus, decrease adverse side effects (Ren et al., 2020).

Several strategies have been applied to non-covalently bind GFs to materials. For example, physical encapsulation, in which a mixture of GFs is incorporated within polymers before their solidification or gelation (Wang et al., 2017), offers a layer of protection for GFs (Mastrullo et al., 2020). Although physical immobilization of GFs can be accomplished under mild conditions at room temperature, only a small fraction of GFs can be bound with this approach and the unpredictable release profiles may also be a problem (Wang et al., 2017). Another example of non-covalent incorporation is adsorption, where GFs are physically immobilized on the surface of different matrices (King & Krebsbach, 2012; Wang et al., 2017). A major drawback of the adsorption method is the difficulty to control the delivery and release rates of multiple GFs (Sharon & Puleo, 2008; Wang et al., 2017).

Layer by layer self-assembly is an alternative approach in which polymers and GFs of opposite charges are coated onto surfaces of varying composition (e.g., glass surface) (Wang et al., 2017). Finally, GFs can also be non-covalently conjugated by affinity binding strategies that rely on the affinity of GFs and extracellular matrix (ECM) components that form part of the biomaterials (Atienza-Roca et al., 2018; Ren et al., 2020). This approach is supported by the natural interactions that happen between heparin-binding domains of ECM proteins and heparin-binding GFs, for example (Atienza-Roca et al., 2018; Martino et al., 2013). Likewise, GFs can be engineered to have a stronger binding to collagen, one of the most common ECM proteins (Ren et al., 2020). Though, the effectiveness of the affinity-based system may depend on the local

ECM composition (Ren et al., 2020). Overall, the common limitations of non-covalent methods are the need to protect GFs from the harsh conditions used in the process to fabricate scaffolds and burst release (Atienza-Roca et al., 2018).

Covalent immobilization of growth factors to biomaterials arises as a promising approach with the potential to improve both stabilization and persistence of delivered growth factors (Masters, 2011; Wang et al., 2017). This strategy is advantageous because it can eliminate the possibility of initial burst release (Masters, 2011; Wang et al., 2017) and the release of GFs depends on the material's degradation rate, which can be controlled (Atienza-Roca et al 2018; Ren et al., 2020).

Chemical or enzymatic crosslinking has been extensively applied to covalently attach GFs to biomaterials through functional residues (Masters, 2011; Ren et al., 2020; Wang et al., 2017). Vascular endothelial growth factor (VEGF) and angiopoientin-1 (Ang1) covalently immobilized to 3D collagen scaffolds increased endothelial cells (ECs) proliferation *in vitro* and infiltration *in vivo* (Chiu & Radisic, 2010). However, although many techniques of covalent conjugation have been created, loss of bioactivity can be a limitation for this method (Wang et al., 2017). Protein fusion is another approach to covalently immobilize GFs to biomaterials (Ren et al., 2020). This strategy has been successfully applied to create materials made of silk fusion proteins that can immobilize both VEGF and basic fibroblast growth factor (bFGF) for tissue engineering applications (Güler et al., 2019; Thatikonda et al., 2018).

1.10 Developing Ubx-based materials to stimulate neovascularization

Because of the unique properties discussed above, Ubx materials can be used in several biomedical applications, including tissue engineering and regenerative medicine, wound healing, biosensors, and drug and gene delivery. Here we will focus on the application of Ubx materials for scaffold neovascularization and therapeutic angiogenesis, which is further explored in Chapter II of this dissertation.

CHAPTER II

PROTEIN-BASED MATERIALS DISPLAYING MULTIPLE GROWTH FACTORS PROMOTE LONG-TERM FORMATION OF FUNCTIONAL BLOOD VESSELS

2.1 Introduction

Blood vessels are essential to supply cells with oxygen and nutrients and to remove waste products (Jain et al., 2005). Due to the diffusion limit of oxygen, cells need to be within 100 to 200 μm of blood vessels in a tissue to survive and function (Carmeliet & Jain, 2000; Jain et al., 2005; Rouwkema et al., 2008). Based on this requirement, stimulating neovascularization to support cell survival is important for critical applications such as wound healing (Atienza-Roca et al., 2018; Demidova-Rice et al., 2012; Jahani et al., 2020; Niu et al., 2019), tissue regeneration and engineering (Atienza-Roca et al., 2018; Filipowska et al., 2017; Jahani et al., 2020; Levenberg et al., 2005; Rouwkema et al., 2008; Rouwkema & Khademhosseini, 2016), and treatment of vascular diseases (Hou et al., 2016; JJ Kim et al., 2016; Mitsos et al., 2012; Simons & Ware, 2003; Xu et al., 2017). The formation of new blood vessels is also essential for scaffolds applied in tissue engineering and regenerative medicine for the integration of the newly formed tissue with the patient's vasculature (Rouwkema & Khademhosseini, 2016; Yao et al., 2020). Furthermore, neovascularization is a necessary and challenging component of tissue engineering strategies as the size of bioengineered constructs can limit the diffusion of oxygen and soluble nutrients available to cells within each construct (Chandra & Atala, 2019; Mastrullo et al., 2020; Yang et al., 2020).

Neovascularization, also known as angiogenesis, is defined as the formation of new blood vessels from preexisting vasculature (Carmeliet, 2000; Lamalice et al., 2007). Creating new blood vessels mainly relies on temporal and spatial delivery of active molecules to develop a structured and functional vascular network (Cao & Mooney, 2007; Kant & Coulombe, 2018; Mastrullo et al., 2020). During angiogenesis, endothelial cells (ECs) respond to local production of pro-angiogenic growth factors (GFs) in the microenvironment and initiate sprouting to form a new vessel (Adams & Alitalo, 2007; Carmeliet & Jain, 2011). The two most highly studied GFs in neovascularization are vascular endothelial growth factor (VEGF) and basic fibroblast growth factor (bFGF) (Augustine et al., 2019; Jain et al., 2005; Mitsos et al., 2012). Both VEGF and bFGF stimulate angiogenesis by activating and promoting EC proliferation, survival, and migration (Carmeliet & Jain, 2011; Duran et al., 2017; Jain, 2003; Mitsos et al., 2012; Ware & Simons, 1997). Another well-described GF known to promote angiogenesis is stromal cell-derived factor 1α (SDF-1α) which binds to endothelial tip cells and stimulates their sprouting (Carmeliet & Jain, 2011; Salcedo et al., 1999). While these GFs are only a partial list of many known to promote angiogenesis, each is well-documented to drive critical aspects of the process.

Many studies have incorporated pro-angiogenic GFs within tissue engineered scaffolds to effectively stimulate angiogenesis *in vivo* or *in vitro* (Kant & Coulombe, 2018; Mastrullo et al., 2020; Novosel et al., 2011). Strategies to deliver GFs to promote neovascularization include non-covalent immobilization within scaffolds, such as physical encapsulation of GFs, absorption of GFs on the surface of a matrix, and layer by layer self-assembly (King & Krebsbach, 2012; Wang et al., 2017). However, burst release of GFs from biomaterials is a key limitation to non-covalent incorporation approaches (Atienza-Roca et al., 2018; Wang et al., 2017). To solve this

problem, GFs are often covalently attached to biomaterials via chemical or enzymatic reactions (Chiu & Radisic, 2010; Wang et al., 2017), photopolymerization (DeLong et al., 2005; Leslie-Barbick et al., 2011), or protein fusion (Güler et al., 2019; Howell et al., 2016; Thatikonda et al., 2018). Some type of effective immobilization is necessary because soluble, free recombinant GFs are unstable, yet cells need to be exposed to GFs for weeks to create mature vessels that will not regress (Niu et al., 2019; Xu et al., 2017). In fact, it has been shown that VEGF needs to be sustainably delivered for about 4 weeks to ensure that the newly induced vasculature is stabilized and persists independently (Gianni-Barrera et al., 2020). Otherwise, if VEGF stimulation is removed too early, the unstable vessels will regress (Dor et al., 2002; Gianni-Barrera et al., 2020). Covalent immobilization can improve the stability and persistence of GFs delivered to cells or tissues (Masters, 2011; Wang et al., 2017). However, for some strategies, covalent conjugation can result in uneven coverage or loss of bioactivity of GFs on biomaterials (Wang et al., 2017). Thus, while GFs are known to be effective, the challenge for their incorporation into biomaterials is creating and maintaining an even, stable, yet active presentation.

Several studies suggest that the incorporation of multiple stable GFs into biomaterials is most effective for promoting angiogenesis. Single GF delivery, especially VEGF alone, may lead to the formation of poorly organized, unstable, and immature blood vessels (Jain, 2003; Mastrullo et al., 2020; Zachary, 2003). Although VEGF is potent at initiating angiogenesis, VEGF (also known as vascular permeability factor or VPF) increases endothelial permeability and creates gaps in endothelial junctions within developing vessels (Carmeliet & Jain, 2011; Dvorak et al., 1995; Zachary, 2003). Because other GFs such as SDF-1α promote barrier formation (Kobayashi et al., 2014), SDF-1α is capable of combatting permeability increases

induced by VEGF and thus would be expected to promote more stable vessel development. The delivery of multiple GFs may be more effective to stimulate the growth of a mature and stable vasculature (Bai et al., 2018; Brudno et al., 2013; Izadifar et al., 2016; Kuttapan et al., 2018; Richardson et al., 2001).

Herein, we immobilize and display GFs using novel protein-based materials composed of the *Drosophila melanogaster* Hox protein Ultrabithorax (Ubx) discovered by our lab (Greer et al., 2009). Ubx self-assembles into films and fibers in mild buffers, creating materials that are cytocompatible, biocompatible and non-immunogenic, and have tunable mechanical properties (Howell et al., 2015; Huang et al., 2010; Patterson et al., 2014; Patterson et al., 2015). GFs can be incorporated into Ubx materials via gene fusion, in which the gene encoding each functional protein is fused to the *ubx* gene without stop codons, thus producing a single polypeptide containing both angiogenic and Ubx proteins. We have previously demonstrated that VEGF alone, when delivered by Ubx materials, is capable of activating and phosphorylating VEGF signaling pathway, through its receptor VEGFR2, to trigger ERK activation and promote angiogenesis (Howell et al., 2016). *In vitro* and *ex vivo* assays confirmed that VEGF-Ubx materials significantly increased the number of ECs that migrate onto materials in response to the presence of active growth factor compared to the control enhanced green fluorescent protein (EGFP)-Ubx (Howell et al., 2016). Furthermore, VEGF-Ubx materials enhanced formation of new blood vessels *in vivo* by 36% using the chick chorioallantoic membrane (CAM) assay (Howell et al., 2016). These results suggest that stimulating neovascularization with VEGF alone may not be sufficient to create mature vasculature and other GFs may aid this process. Here we describe our strategy to simultaneously covalently incorporate and stabilize VEGF, SDF-1α, and

bFGF into protein-based materials to induce neovascularization *in vivo*. These GFs were chosen because they promote the development and stabilization of functional blood vessels in a synergistic manner by performing different functions. In this study, we tested whether protein fusions composed of VEGF, SDF-1α, and bFGF genetically fused to Ubx (VSF-Ubx) can activate ECs to migrate and rescue cell survival with *in vitro* migration and viability assays. Furthermore, fibers composed of VSF-Ubx were able to stimulate and guide neovascularization after subcutaneous implantation in mice, demonstrating that VSF-Ubx materials can promote the formation of stable, mature vasculature *in vivo*.

2.2 Results and Discussion

The goal of this study is to test if materials that display a combination of active VEGF, bFGF, and SDF-1α induce and guide neovascularization responses *in vitro* and *in vivo*. We have genetically fused VEGF, bFGF, and SDF-1α to Ubx, a protein that self-assembles into biomaterials (Greer et al., 2009; Huang et al., 2011; Tsai et al., 2015). Ideally, these fusion proteins will also self-assemble into materials and retain the GFs in an active and stable state. A second negative control was created in which maltose binding protein (MBP) was fused to Ubx due to its ability to increase protein solubility (Tsai et al., 2015). Finally, Ubx, VEGF-Ubx, bFGF-Ubx, and SDF-1α-Ubx were all fused to enhanced green fluorescent protein (EGFP) to both boost yield and enable fiber visualization (Figure 4). Importantly, none of the fusions reported herein impede materials assembly, producing Ubx fibers with uniform morphology (Tsai et al., 2015) (Figure 5).

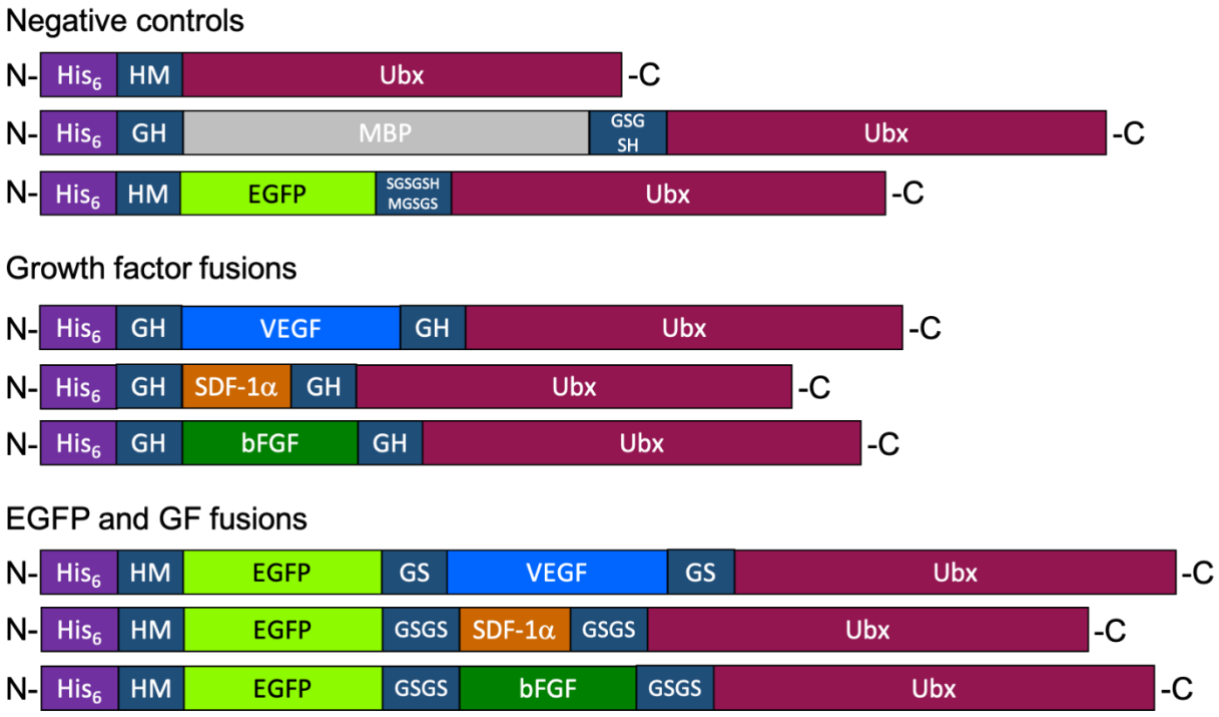

Figure 4. Schematic representation of all fusion proteins used in this study.
All of the constructs contain a Histidine tag on the N-terminus for protein purification (purple box), followed by a linker (navy blue box), the functional protein, another linker (navy blue box), and Ubx protein (maroon) on the C-terminus. Note that the linking amino acid sequence between MBP and Ubx proteins is GSGSH, and between EGFP and Ubx is SGSHMGSGS.

The second concern is whether the GFs will retain their activity once fused to Ubx. We have previously extensively tested both VEGF-Ubx and a double fusion, EGFP-VEGF-Ubx, and found that VEGF is active in materials made from either fusion (Howell et al., 2016). However, the structures of both SDF-1α and bFGF differ from VEGF. Importantly, the N-terminus, which is fused to the his-tag, and the C-terminus, which is fused to Ubx, are both placed differently relative to the receptor binding interface in these growth factors (Figure 6). Thus, even though the VEGF strategy was successful, these fusions may prevent other GFs from dimerizing or retaining activity in Ubx materials. To test the activity of each of the GFs in Ubx materials, we

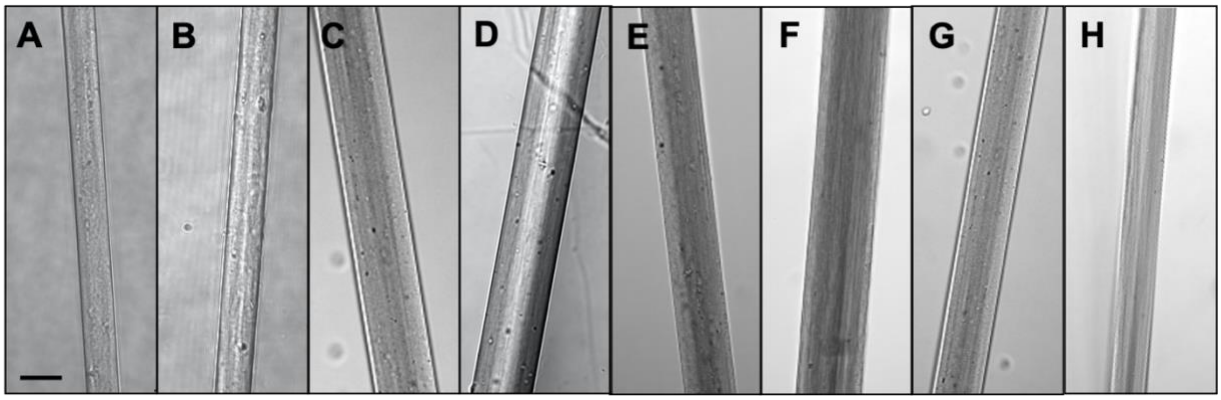

Figure 5. Materials formation and fiber morphology are not significantly impacted by protein fusions.
Differential interference contrast (DIC) microscopy of fibers composed of MBP-Ubx (A), SDF-1α-Ubx (B), bFGF-Ubx (C), VEGF-Ubx (D), EGFP-Ubx (E), EGFP- SDF-1α-Ubx (F), EGFP- bFGF-Ubx (G), and EGFP- VEGF-Ubx (H). Scale bar represents 10 μm.

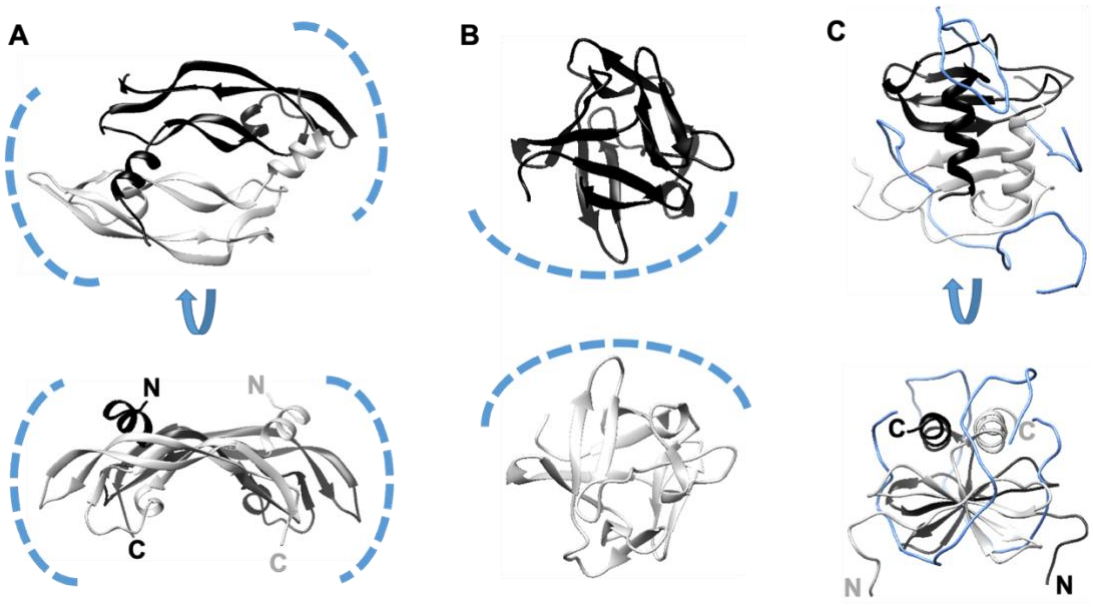

Figure 6. Schematic representation of the structures of each growth factor used.
VEGF (A), bFGF (B), and SDF-1α (C) are shown as 2 monomers (one black and one gray). The location of the receptor binding interface is depicted as blue dashed lines (A, B) or as the backbone (blue lines) of the receptor (C). Schematic created with Chimera Software (UCSF).

performed a migration assay with human umbilical vascular endothelial cells (ECs). Because GFs activate and stimulate endothelial cells (ECs) to migrate, we can use migration to test whether GFs in Ubx materials are active or not in the absence of serum. In this assay, ECs were incubated in normal growth medium to reach confluency, then transferred to basal media without serum and serum starved for 6 hours. Following serum starvation, Ubx fibers with or without GFs were placed on a confluent monolayer of ECs overnight to allow cells to respond to GFs within the materials. Cells were fixed and analyzed using confocal microscopy. When presented in soluble form, GFs stimulate cell migration to different degrees. We tested increasing concentrations of each GF and found significant differences between the average number of ECs that migrate to the control fibers, composed of MBP-Ubx, and the Ubx materials composed of 100% of VEGF (Figure 7A), 100% of SDF-1α (Figure 7B), and 100% of bFGF (Figure 7C). Data for VEGF-Ubx fibers were comparable to our prior report (Howell et al., 2016). Therefore, this result shows that all 3 GFs retain activity when immobilized in Ubx materials and promote dose-dependent increases in EC migration. Our results indicate that SDF-1α is less effective at stimulating EC migration than either VEGF or bFGF, which may be caused by its tertiary structure affecting the activation of materials or because SDF-1α is possibly a less potent activator of angiogenesis than the other GFs tested.

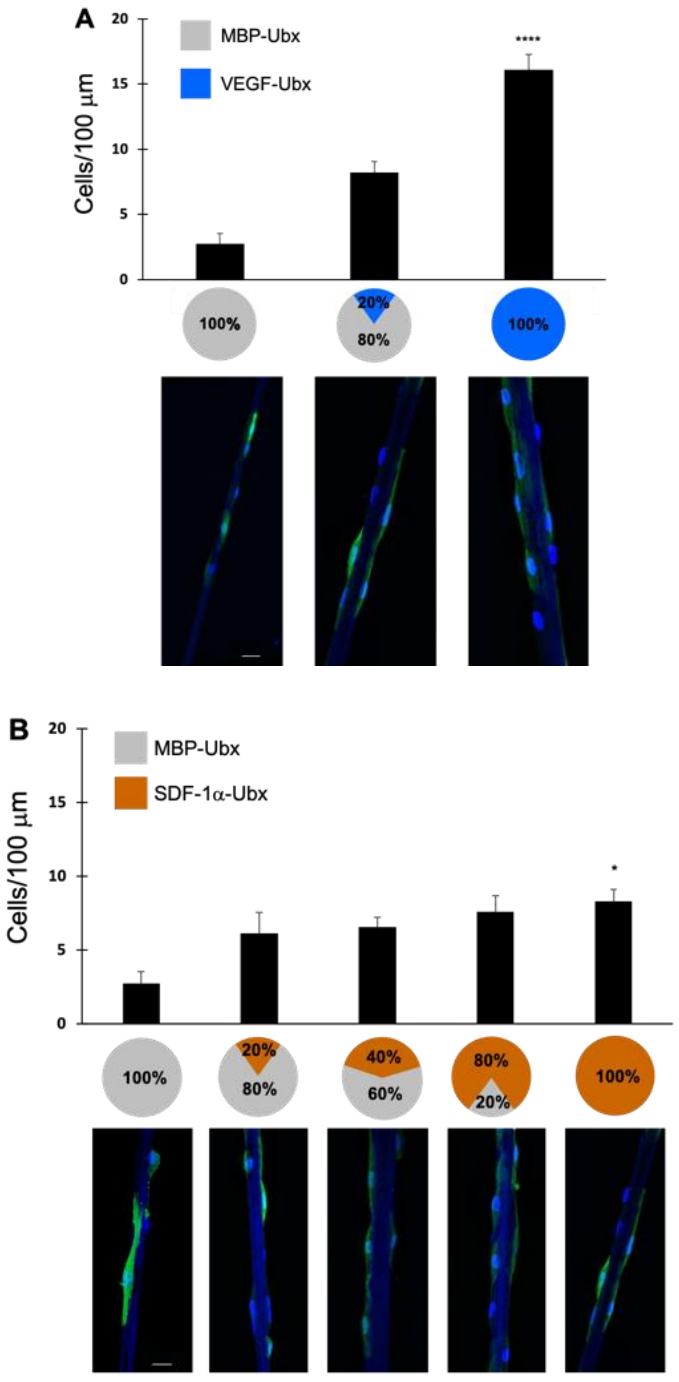
A
MBP-Ubx
VEGF-Ubx
Cells/100 µm
20
15
10
5
0
****
100%
20%
80%
100%
B
MBP-Ubx
SDF-1α-Ubx
Cells/100 µm
20
15
10
5
0
*
100%
20%
80%
40%
60%
80%
20%
100%

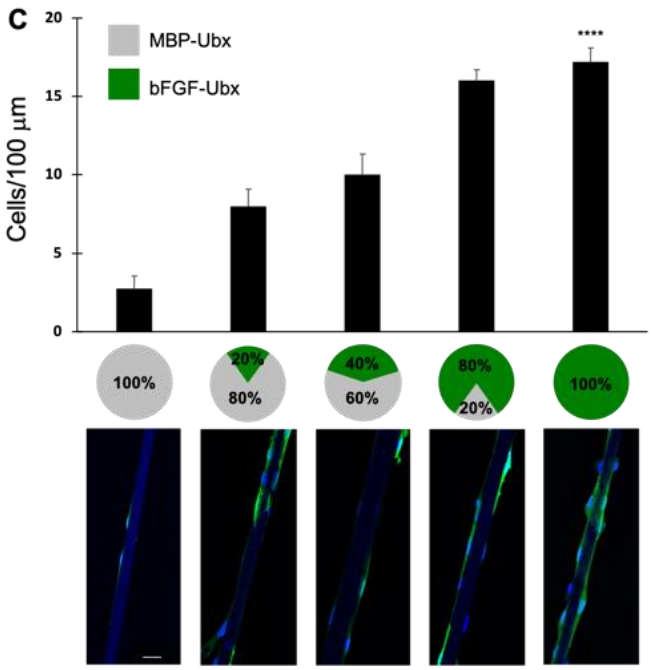

Figure 7. GFs remain active when immobilized in Ubx materials and promote dose-dependent EC migration.
ECs were serum starved for 6 hours and then incubated with fibers composed of varying combinations of MBP (negative control) and GFs as indicated in each panel. Data represent the average number of ECs that migrate onto (A) VEGF-Ubx, (B) SDF-1α-Ubx, and (C) bFGF-Ubx materials. A greater number of cells migrate to fibers composed of 100% of each GF compared to the negative control MBP-Ubx fiber. Migration assays were quantified by counting the number of cell nuclei in a 100 µm length of fiber ($n = 3$ independent experiments). Scale bars indicate 10 µm. Statistics were obtained by one-way ANOVA with Dunnett's multiple comparison tests. * $p < 0.05$, **** $p < 0.0001$ compared to the control MBP-Ubx.

Neovascularization is a complex, multi-step process that involves many GFs to build a mature and stable blood vessel. A combinatorial delivery of GFs has the potential to improve the activation of GF receptors and induce cell behaviors required for different steps of angiogenesis. Thus, aiming to further increase the EC response, we monitored EC migration following incubation with fibers composed of different combinations of VEGF, SDF-1α, and bFGF, with or without MBP. This approach is possible because fusions do not impact Ubx assembly into materials (Tsai et al., 2015). We started with mixtures containing 20% VEGF, as its activity is

similar to established physiological concentrations of soluble VEGF utilized by other *in vitro* studies (Howell et al., 2016). Using the same migration assay described above, we observed a synergistic effect on EC migration with the presence of more than one GF. For instance, fibers composed of 20% VEGF and 20% SDF-1α (Figure 8) stimulate migration better than fibers composed of 20% VEGF (Figure 7A) or 100% SDF-1α (Figure 7B). Also, migration stimulated by fibers composed of 20% VEGF and 20% FGF (Figure 8) is nearly double the response seen with fibers composed of 20% VEGF (Figure 7A) or 20% FGF (Figure 7C). Fibers containing 40% bFGF and 40% SDF-1α (Figure 8) elicited a higher EC response than 100% of each GF alone (Figure 7). The highest levels of cell migration were seen with Ubx materials composed of the mixture of GFs containing 20% VEGF-Ubx, 40% SDF-1α-Ubx, and 40% bFGF-Ubx (hereafter referred to as $V^{20}S^{40}F^{40}$) (Figure 8).

Because cells require GFs to survive and function, we further tested if GFs displayed by Ubx materials are sufficient to maintain EC viability under starvation conditions. We performed a viability assay in which ECs were directly seeded onto Ubx fibers and cultured in growth medium to allow the cells to attach to materials for 16 hours. The media was then replaced with basal media without GFs and cells were serum starved for 8 hours. At this point, only cells in contact with GF-Ubx fibers have access to GFs. The number of cells attached to Ubx fibers was recorded before and after serum starvation. The average number of cells present on fibers composed of MBP-Ubx, used as control, was significantly lower compared to each single GF, showing that each GF can induce cell survival when immobilized on Ubx fibers (Figure 9). Likewise, a significantly higher number of ECs remained attached to fibers composed of combinations of GFs at different ratios, indicating that cell responsiveness can also be achieved

with GFs mixture (Figure 9). Therefore, these results confirm that presentation of GFs withing Ubx fibers maintains EC viability during serum starvation.

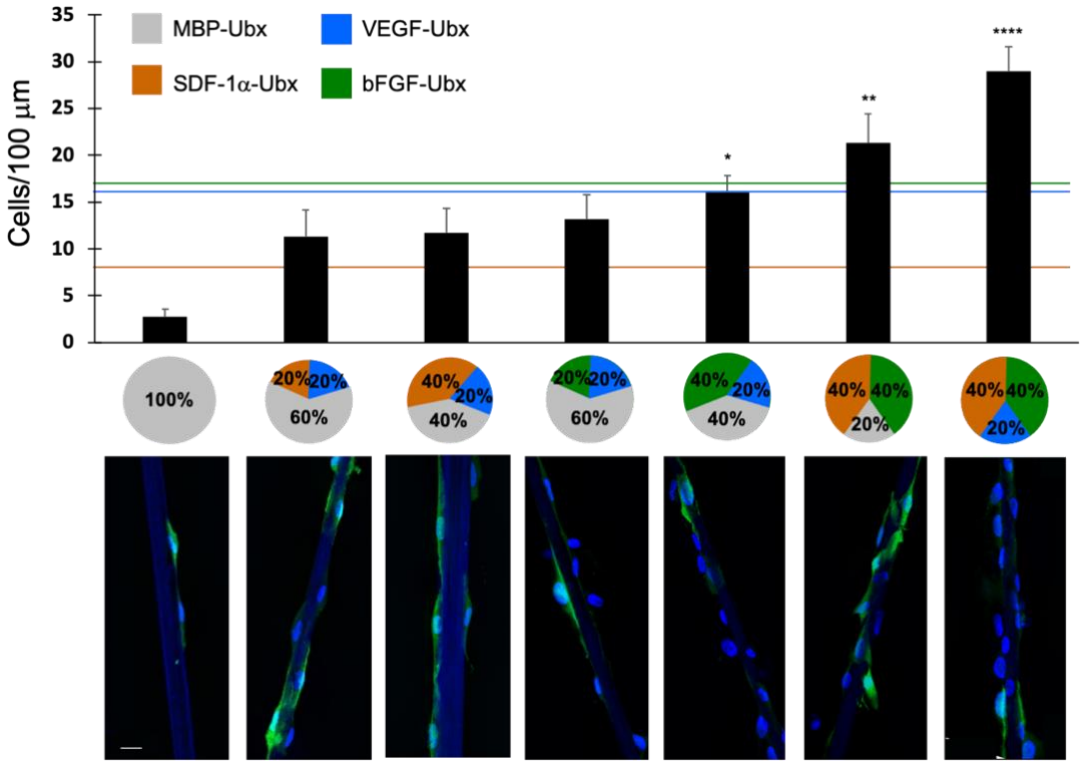

Figure 8. Fibers displaying combinations of GFs are more effective at promoting cell migration than fibers harboring a single GF.
The indicated concentrations of GFs were tested for the ability to improve EC migration onto fibers compared to a negative MBP-Ubx control. Migration assays were quantified by counting the number of cell nuclei in a 100 µm length of fiber ($n = 3$ independent experiments). *Top*, average number of cells that migrate onto fibers displaying different combinations of GFs as indicated in the pie charts (*middle*). *Bottom,* a representative image of cells (green) migrating onto fibers for each combination is shown beneath its respective pie chart. Horizontal lines colored to match each GF indicate the number of cells per 100 µm that migrate to fibers composed of 100% of each GF based on data from Figure 7. Scale bar indicates 10 µm. Statistics were obtained by one-way ANOVA followed by Dunnett's multiple comparison tests. * $p < 0.05$, ** $p < 0.01$, **** $p < 0.0001$ compared to the control MBP-Ubx.

We next investigated if GFs-Ubx materials induce and guide neovascularization *in vivo.* Using a mouse model, sterile PVA sponges wrapped with Ubx fibers were implanted subcutaneously. To facilitate materials visualization, fibers composed of either EGFP-Ubx, as a negative control, or EGFP- $V^{20}S^{40}F^{40}$-Ubx were used in this experiment (Figure 10A). After 2 weeks of implantation, sponges and tissues were harvested and underwent a tissue clearing and immunolabeling process to quantify the formation of new blood vessels adjacent to Ubx materials. Whole mounts were imaged by confocal microscopy, in which different fields around the sponges were captured and a double-blinded scoring analysis was performed for each image. Responses from each implant were analyzed by quantifying blood vessels that formed adjacent to Ubx materials. Gross examination of implants suggested a difference between control (EGFP-Ubx) and treatment groups (EGFP-$V^{20}S^{40}F^{40}$-Ubx), where the latter materials appeared to more robustly stimulate the formation of new vessels (Figure 10B, C). Representative images from confocal analyses illustrate that blood vessel formation (magenta signal) occurred adjacent to Ubx materials (green signal) in EGFP-$V^{20}S^{40}F^{40}$-Ubx samples, but not in EGFP-Ubx controls (Figure 10D, E). Blinded quantification of blood vessel formation adjacent to Ubx materials revealed a significantly higher percentage of events where blood vessels formed adjacent to EGFP-V20S40F40-Ubx materials versus control EGFP-Ubx materials (Figure 2-7F). These results show that Ubx materials present active GFs to promote angiogenic blood vessel growth 2 weeks after subcutaneous implantation in vivo.

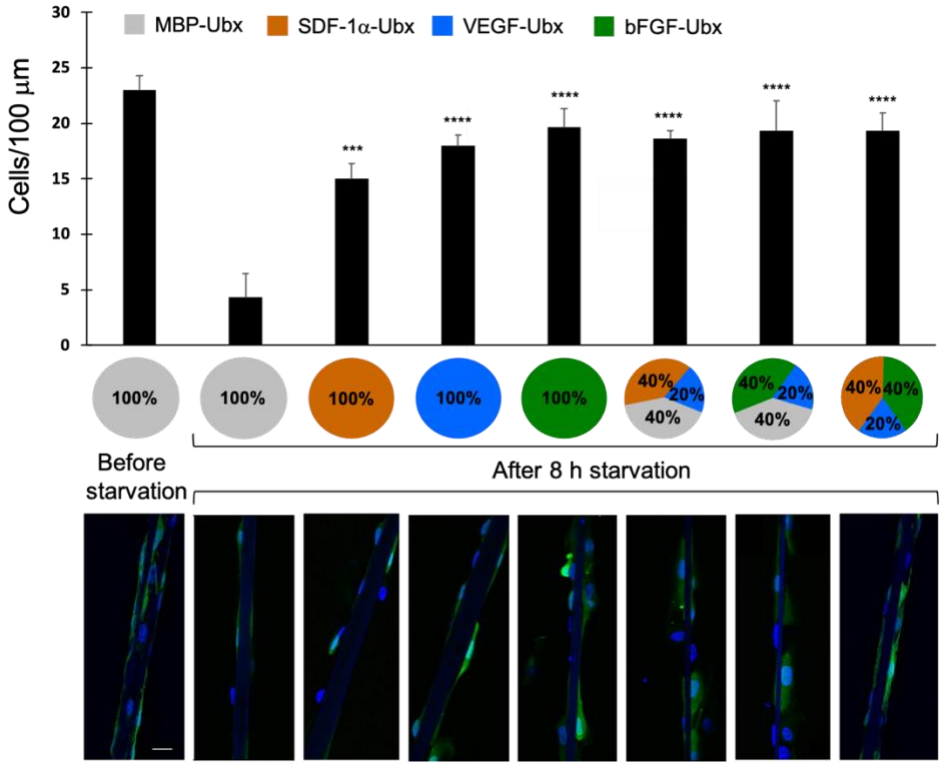

Figure 9. Fibers displaying GFs successfully rescue cell viability after serum starvation. ECs attached to Ubx fibers were subjected to serum starvation for 8 hours to test for the ability of GFs to maintain cell survival. *Top,* the average number of cells attached to each fiber was recorded before starvation and no significant differences were seen across the experiment (not shown). The number of cells that were present on fibers after the 8-hour starvation is significantly higher on the materials displaying GFs alone or in combination compared to the negative control. *Bottom,* representative images illustrating EC survival on each formulation of Ubx. Viability assays were quantified by counting the number of cell nuclei in a 100 µm length of fiber ($n = 3$ independent experiments). Scale bar represents 10 µm. Statistics were obtained by one-way ANOVA followed by Dunnett's multiple comparison tests. *** $p < 0.001$, **** $p < 0.0001$ compared to the control MBP-Ubx.

To build a functional vasculature, vessels must become mature and stable with time. Prior studies show that removal of GF stimulation can regress newly formed vessels (Gianni-Barrera et al., 2020). To assess whether EGFP-$V^{20}S^{40}F^{40}$-Ubx materials are effective beyond two weeks of implantation and promote vessel maturation *in vivo*, sponges wrapped with Ubx fibers were

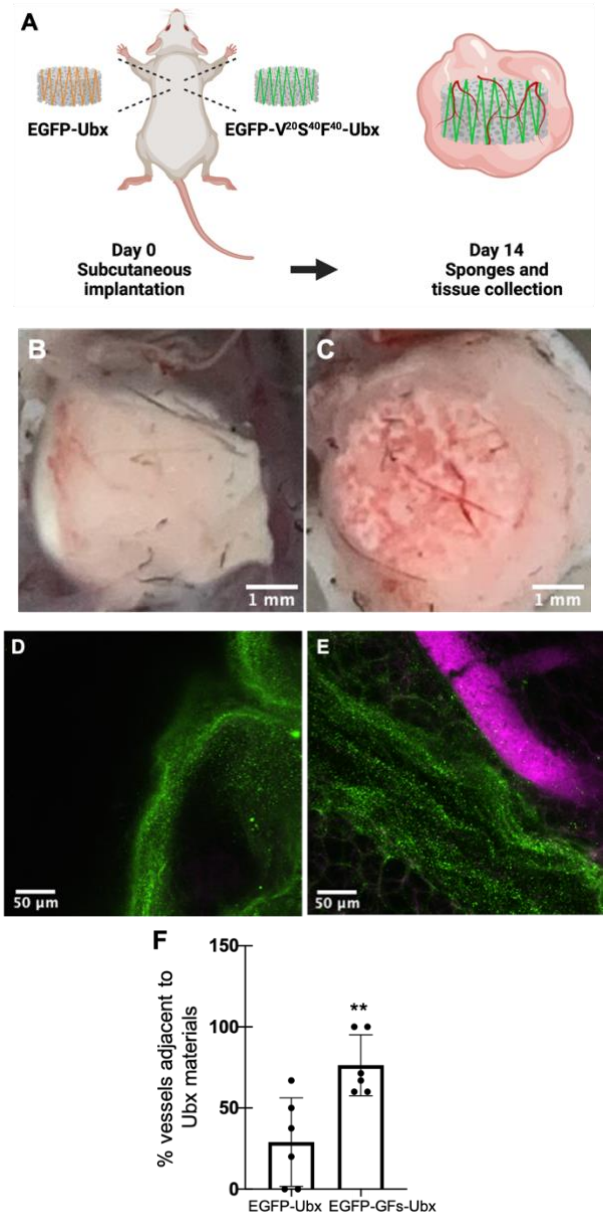

Figure 10. $V^{20}S^{40}F^{40}$-Ubx materials promote and guide neovascularization in vivo.
To test the ability of Ubx materials displaying multiple GFs to stimulate blood vessel formation, sponges wrapped with Ubx fibers with and without GFs were implanted in mice. A) Schematic representation of our mouse model, in which sterile PVA sponges were coated with EGFP-Ubx fibers, as control, or EGFP-$V^{20}S^{40}F^{40}$-Ubx fibers, then subcutaneously implanted in mice for two weeks, followed by tissue clearing and vessel quantification. Schematic created with BioRender. Images of control (B) and $V^{20}S^{40}F^{40}$ sponges (C) after collection suggest increased *in vivo* neovascularization in response to $V^{20}S^{40}F^{40}$-Ubx materials. Scale bars are 1 mm. Representative images of EGFP-Ubx (D) and EGFP-$V^{20}S^{40}F^{40}$-Ubx (E) samples with Ubx materials following immunofluorescence staining for Ubx (green). Blood vessels are detected by autofluorescence (magenta). Scale bars indicate 50 µm. F) Statistical analysis confirms a significant difference between EGFP-Ubx and EGFP-$V^{20}S^{40}F^{40}$-Ubx samples, reported as the percentage (%) of new blood vessels growing adjacent to Ubx materials (n = 6 mice). Statistics were obtained with unpaired two-tailed Student's t test, ** $p < 0.01$.

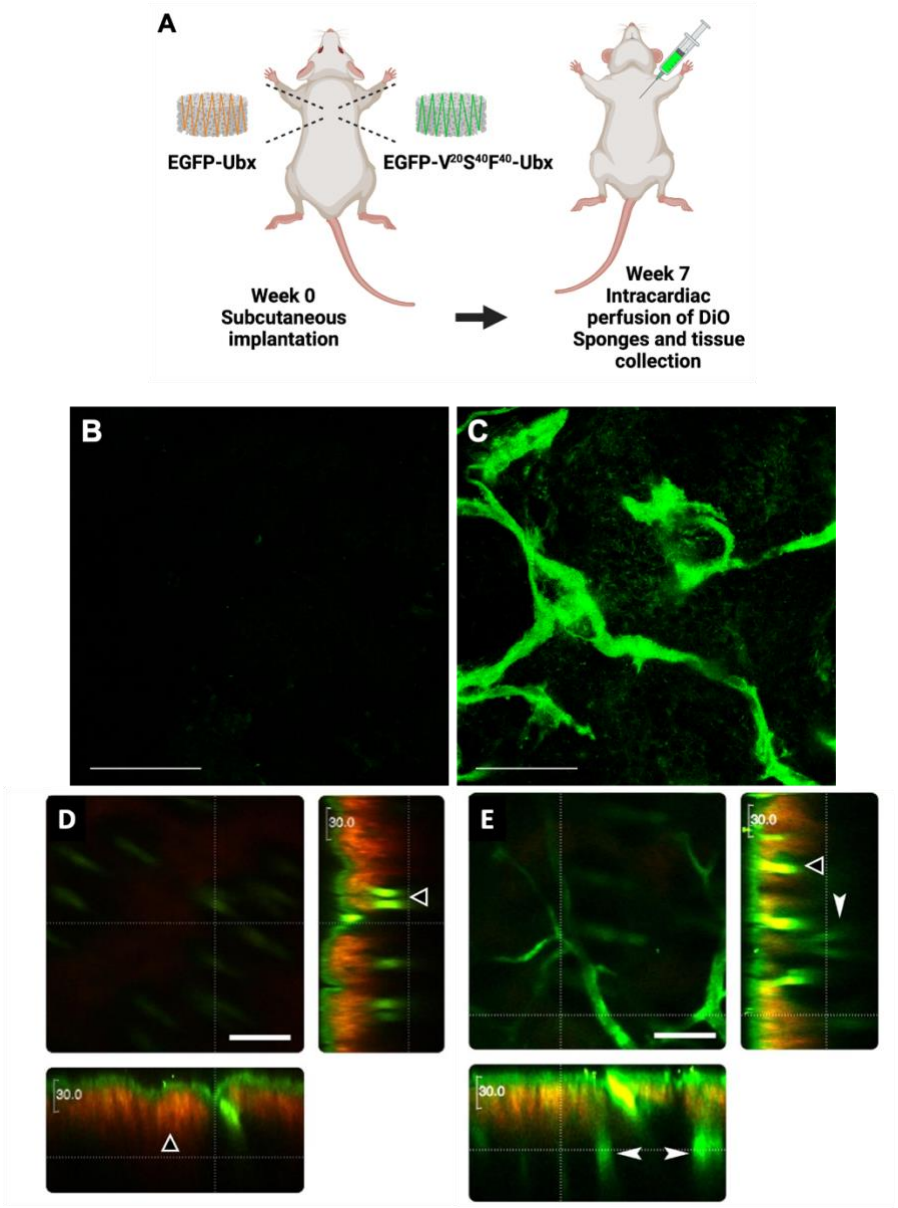

Figure 11. $V^{20}S^{40}F^{40}$-Ubx materials induce the formation of mature, functional vasculature following long term implantation.

Sponges wrapped with $V^{20}S^{40}F^{40}$-Ubx and EGFP-Ubx fibers were subcutaneously implanted in mice for 7 weeks prior to intravenous injection of DiO. A) Schematic representation of the approach, in which sterile PVA sponges were wrapped with EGFP-Ubx fibers, as control, or $V^{20}S^{40}F^{40}$-Ubx fibers, then subcutaneously implanted for 7 weeks prior to intracardiac perfusion to deliver DiO. Schematic created with BioRender. Representative images collected using confocal microscopy for (B) EGFP-Ubx and (C) $V^{20}S^{40}F^{40}$-Ubx. Two photon fluorescence was additionally used to analyze subcutaneous perfusion of vessels for (D) EGFP-Ubx and (E) $V^{20}S^{40}F^{40}$-Ubx materials. Tissue autofluorescence indicated by open arrowheads. White arrowheads indicate new and patent blood vessels in both X and Y axis on the right panel. All scale bars represent 50 μm.

implanted in mice for 7 weeks (Figure 11A). Animals were then perfused with DiO, a green, fluorescent dye, before tissue fixation. While green fluorescence (indicative of DiO perfusion) of newly formed blood vessels was difficult to detect in EGFP-Ubx controls (Figure 11B), perfusion was readily observed in implants receiving EGFP-$V^{20}S^{40}F^{40}$-Ubx fibers (Figure 11C). Additional analyses using two photon fluorescence confirmed this observation with few vessels perfused with DiO in EGFP-Ubx control group, but continuous perfused network visible in EGFP-$V^{20}S^{40}F^{40}$-Ubx treatment group (Figure 11E). These results confirm the formation of patent blood vessels induced by EGFP-$V^{20}S^{40}F^{40}$-Ubx compared to EGFP-Ubx controls.

2.3 Conclusions

In the present work we demonstrate that VEGF, bFGF, and SDF-1α each retain activity when genetically fused to Ubx protein and assembled into materials, despite the different three-dimensional structures and receptor interfaces of each protein. Furthermore, our *in vitro* data confirm that EC response to GFs is dose dependent. We have also showed a synergistic effect of multiple GFs on HUVECs incubated with Ubx fibers, when compared to control (MBP-Ubx).

Our strategy further demonstrates that Ubx materials can be used to safely and effectively induce neovascularization *in vivo* by displaying multiple GFs. The presented data shows that functional blood vessels successfully formed in co-localization with GFs-Ubx materials within two weeks. Furthermore, we show that the newly formed vasculature persists for up to 7 weeks, confirming that GFs-Ubx fibers promote vessel maturation. Finally, our results also indicate that after 7 weeks of materials implantation the vessels are patent.

This work expands the number of protein biomaterials that retain protein function and activity after incorporation by gene fusion. Many other studies have used other strategies to deliver GFs, such as physical entrapment or chemical crosslinking, to promote angiogenesis. Our study demonstrates that multiple GFs retain their function and are stabilized when genetically fused to Ubx, which self-assembles into materials. Therefore, our results demonstrate that gene fusion can be generally applicable to functionalize protein-based materials. Overall, we anticipate the potential applications of these biomaterials for diabetic wound healing, vascularization of bioengineered tissues, and treatment of vascular diseases.

2.4 Materials and Methods

Construction of plasmids. Fusion proteins composed of MBP, VEGF, SDF-1α, bFGF, and EGFP-VEGF fused to Ubx were constructed as previously reported (Tsai et a., 2015). A new universal construct was created in which a longer, flexible linker was inserted between EGFP and Ubx, and NdeI cut site 5' to EGFP was deleted. SDF-1α and bFGF cut from single growth factor plasmids were inserted into the new universal vector to create EGFP- SDF-1α-Ubx and EGFP-bFGF-Ubx fusions.

Ubx protein expression and purification. Monomers of his-tagged Ultrabithorax splicing isoform Ia, either alone or fused to MBP, VEGF, SDF-1α, bFGF, EGFP-VEGF (Tsai et al., 2015), EGFP, EGFP-SDF-1α, or EGFP-bFGF were produced in *E. coli* as previously described (Patterson et al., 2014). DNA sequences encoding all protein fusions were inserted into the NdeI

site of pET19b-Ubx, between the sequences encoding the N-terminal His-tag and Ubx, before transformation into Rosetta™(DE3)pLysS competent cells (Novagen). A single colony was used to inoculate 100 mL of Luria broth with 50 mg/L carbenicillin and 30 mg/L chloramphenicol. Overnight liquid cultures (7 mL) were inoculated into 1 L Luria broth with the same antibiotics. Protein expression was induced at mid-log phase with $OD_{600\ nm}$ ~0.6 with 1 mM isopropyl-β-D-1-thiogalactopyranoside (IPTG) for 4 to 5 hours at 16 °C. Cells were harvested by centrifugation at 3,500 x g for 30 minutes or 17,568 x g for 10 minutes at 4 °C and stored at −20 °C. To purify Ubx and Ubx fusion proteins, cell pellets derived from 2L of cell culture were lysed in 40 mL of lysis buffer containing 50 mM NaH_2PO_4, 5% glucose (w/v), and 500 mM NaCl (Buffer G) at either pH 8.0 or pH 8.3, with two ethylenediaminetetraacetic acid-free protease inhibitor tablets (Roche), 0.18 mg/mL DNase I (Roche), 0.2 mg/mL lysozyme (Sigma), 5 mM dithiothreitol (DTT; ThermoFisher), and 1.5 mM phenylmethylsulfonyl fluoride (PMSF; MilliporeSigma). Cell debris was removed by centrifugation for 30 minutes at 35,000 x g or 24 minutes at 33,746 x g at 4 °C. Ubx protein was purified from the clarified cell lysate by nickel-nitrilotriacetic acid chromatography (ThermoFisher) as follows. The supernatant was loaded onto a column formed from 4 mL of resin slurry (ThermoFisher) that was previously equilibrated with 100 mL of equilibration buffer (50 mM NaH_2PO_4, 5% glucose (w/v), 500 mM NaCl, at pH 8.0). The column was washed with 50 mL of equilibration buffer followed by 50 mL of equilibration buffer containing 20 mM imidazole (pH 8.0), then washed with 7.5 mL of equilibration buffer containing 100 mM imidazole (pH 8.0). Finally, the purified protein was eluted in 15 mL of elution buffer (300 mM imidazole dissolved in equilibration buffer at pH 7.0).

Ubx materials production. Purified Ubx and Ubx fusion proteins were diluted into a shallow buffer reservoir containing 50 mM NaH_2PO_4, 500 mM NaCl, and 5% glucose w/v, at pH 8.0 for materials formation as previously described (Howell et al., 2016; Huang et al., 2011). Fibers were drawn from film that forms at the air-water interface and wrapped around 5 mm sterile plastic inoculation loops (Mendes et al., 2018) and stored in a sterile tissue culture dish with humidity until use within one day.

Cell culture. Primary human umbilical vein endothelial cells (HUVECs; Lonza, C2517A) transformed with lentivirus delivering EGFP (Bayless et al., 2009; Patterson et al., 2014; Patterson et al., 2015) were cultured and used at passages 3-6. Cells were grown on gelatin-coated tissue culture flasks, passaged once per week in M199 growth medium supplemented with heparin, bovine hypothalamic extract, 10% fetal bovine serum, antibiotics, and gentamycin as previously described (Bayless et al., 2009).

Migration assay. HUVECs expressing EGFP were seeded onto gelatin-coated wells and allowed to reach confluency. Cells were then cultured in M199 either without serum or with low (1%) serum for 6 hours prior to placement of inoculation loops wrapped with fibers composed of MBP-Ubx, VEGF-Ubx, SDF-1α-Ubx, bFGF-Ubx or combinations of different growth factors onto cell monolayers. Cells and loops wrapped with fibers were cultured overnight with 250 μL of M199 media supplemented with 1.5% serum to allow cells to migrate to fibers. After a 16-hour incubation, cells on Ubx fibers were fixed by removing media and adding 250 μL of a freshly made 4% paraformaldehyde (PFA) solution in PBS (16 mM Na_2HPO_4, 2.6 mM KCl, 1.2 mM K_2HPO_4, 68 mM NaCl). Cells were counterstained with 10 mM 4',6-diamidino-2-

phenylindole (DAPI; Molecular Probes), placed on a 22 mm X 55 mm coverslip and imaged immediately using confocal microscopy on a Nikon Eclipse Ti equipped with NIS Elements AR 4.10.01 software. Migration assays were quantified by counting the number of cell nuclei attached to a 100 μm section of fiber.

Cell viability assay. Fiber-wrapped loops directly seeded with 35,000 cells suspended in 250 μL of growth media were cultured overnight so that cells could attach to Ubx fibers. Growth medium was aspirated, and cells cultured on Ubx fibers were starved for 8 hours in M199 media without serum, then fixed using 4% PFA as described above. The EGFP HUVECs were counterstained with 10 mM 4',6-diamidino-2-phenylindole (DAPI; Molecular Probes), placed on a 22 mm X 55 mm coverslip and imaged immediately using confocal microscopy on a Nikon Eclipse Ti equipped with NIS Elements AR 4.10.01 software. Cell viability assays were quantified by counting the number of cell nuclei in a 100 μm length of fiber.

Ubx implantation in mice. PVA sponges (10 mm diameter, 1 mm thick disks) were obtained from PVA Unlimited (Warsaw, IN) and prepared according to the method described by Molecular Imaging Research (Standard Operating Procedures, Sponge Granuloma in Rats, August 2008) (Patterson et al., 2015). Briefly, sponges were cut with a sterile dermal punch into 4 mm diameter disks, soaked in 70% EtOH overnight, rinsed in sterile filter-purified water (autoclaved Millipore Milli-Q) followed by sterile PBS (16 mM Na_2HPO_4, 2.6 mM KCl, 1.2 mM K_2HPO_4, 68 mM NaCl), and stored in sterile water at 4 °C overnight. Hydrated sterile sponges were transferred to a sterile Petri dish. Fibers and films composed of 20% VEGF-Ubx, 40%

SDF-1α-Ubx, and 40% bFGF-Ubx fusions and plain Ubx or EGFP-Ubx (controls) were wound around the sponge (12-15 wraps per sponge) using a sterile hemostat to hold the sponge. The fiber-coated sponges were stored for less than 24 hours in sterile PBS (16 mM Na_2HPO_4, 2.6 mM KCl, 1.2 mM K_2HPO_4, 68 mM NaCl) to prevent dehydration prior to implantation. Subcutaneous implantation of fiber-wrapped sponges was performed using 8-10-week-old Sv129 mice. All mice were anesthetized before making a small midline incision on the dorsal surface between the scapulae of each mouse. Sponges were placed in the subcutaneous space with one control sponge (wrapped in plain Ubx or EGFP-Ubx) on one side of the incision and one sponge wrapped in GFs-Ubx materials on the other. The incision was closed with sutures and mice were housed separately and monitored closely for the following 48 hours.

Tissue clearing and quantifying angiogenic responses. After 2 weeks, implanted mice (n = 6) were euthanized with CO_2. Sponges coated with Ubx materials and surrounding skin were harvested and fixed in 4% paraformaldehyde (PFA) in PBS overnight at 4 °C. Tissues were processed using the immunolabeling-enabled three-dimensional imaging of solvent-cleared organs (iDISCO) technique (Renier et al., 2014; Rouger et al., 2016). Fixed samples were dehydrated using a gradient of methanol (50%, 75%, 100%) diluted in PBS, incubating for 1 hour per methanol solution at room temperature. Samples were then incubated overnight at 4 °C in an ice-cold mixture of 70% methanol (ThermoFisher), 20% dimethylsulfoxide (DMSO; Sigma), and 10% hydrogen peroxide (Sigma) to reduce tissue autofluorescence. Samples were rehydrated at room temperature with methanol solutions in PBS (75%, 50%, and PBS) for 1 hour per solution, and blocked at room temperature for 12 hours in blocking solution (1% BSA, 0.2% sodium azide, 1X TBS, 1% goat serum, 0.1% Triton-X). For visualization of Ubx materials,

samples were stained with rabbit anti-GFP primary antibody (Lee et al., 2009) diluted 1:1000 in blocking solution for 48 hours at 37 °C. Samples were then washed for 12 hours in 0.1% Triton-X in PBS and subsequently incubated in goat anti-rabbit Alexa Fluor® Plus 647 secondary antibody (Invitrogen) diluted 1:600 in blocking solution for 36 hours at 37 °C. Samples were washed for 12 hours with 0.1% Triton-X in PBS at room temperature, then transferred to PBS and kept at 4 °C until clearing. To clear the samples, immunolabeled tissues were dehydrated by incubating in a tetrahydrofuran (THF; Sigma) gradient (50%, 75%, and 100%) diluted in double distilled water (Millipore Milli-Q) at room temperature for 1 hour per solution. Finally, samples were incubated in dibenzyl ether (DBE; Sigma) overnight, changing solutions until samples were completely clear, and stored immersed in DBE at room temperature prior to imaging using an Olympus FLUOVIEW FV3000 Confocal Laser Scanning Microscope. For all of the steps described, samples were incubated on lab rotators. Ubx materials were imaged at 647 nm wavelength so that we could rely on red blood cell autofluorescence to identify blood vessels at 561 nm wavelength (H Li et al., 2020; Taniguchi, 2017; Whittington & Wray, 2017). A total of 72 images, an average of 6 images per sponge, were analyzed regarding the presence of blood vessels adjacent to Ubx materials, and a blinded scoring was performed by 4 observers.

Vessel patency associated with long term implants. To determine if patent vessels formed in mice receiving Ubx materials after 7 weeks, mice (n = 6) were euthanized with CO_2 and perfused slowly following intracardiac puncture with 10 mL PBS, 5 mL DiO (120 µg/mL), and 10 mL 4% PFA in PBS. The sponges and adjacent skin tissues were excised and placed in 1 mL of 4% PFA in PBS overnight. Samples were washed three times, mounted in Fluoro-Gel

mounting medium (Electron Microscopy Sciences), and imaged using a non-linear optical microscopy–optical coherence microscopy (NLOM–OCM) combined system (Bai et al., 2014).

Statistical analysis. All data are presented as the mean and standard deviation, averaged from 3 individual measurements for *in vitro* data or 6 images per sponge for mice data. Statistical analyses were performed using Prism 9 (GraphPad Software, USA). *p*-Values less than 0.05 were considered statistically significant.

CHAPTER III

THE CHICK CHORIOALLANTOIC MEMBRANE (CAM) AS A MODEL TO STUDY NEOVASCULARIZATION INDUCED BY UBX MATERIALS

3.1 Introduction

The chick chorioallantoic membrane (CAM) is a highly vascularized extraembryonic membrane formed during embryonic development by the fusion of the allantois and chorion (Marshall et al., 2020; Nowak-Sliwinska et al., 2014). These structures are responsible for functions such as gas exchange and waste product removal (Nowak-Sliwinska et al., 2014; Ribatti, 2012), similarly to the mammalian placenta (Marshall et al., 2020; Nowak-Sliwinska et al., 2014). The CAM's extensive vascularization has allowed it to be used experimentally; the first study using CAM was reported in 1911 and utilized this membrane to demonstrate growth of a transplanted tumor (Rous & Murphy, 1911). Several decades later, the CAM has been widely applied and a well-established *in vivo* model to study angiogenesis and vascular responses (Auerback et al., 1974; Ausprunk et al., 1974; Ribatti et al., 1997).

The CAM assay is simplistic, cost-effective (Moreno-Jiménez, et al., 2017; Nowak-Sliwinska et al., 2014; Ribatti et al., 1997; Ribatti, 2012) and allows for direct observation of nascent vessels (Ribatti et al., 1997) in a short-term, insentient system (Moreno-Jiménez, et al., 2017). Additionally, the widespread availability of fertilized chicken eggs, ease of embryo visualization (Nowak-Sliwinska et al., 2014), and assay reproducibility make this technique advantageous (Nowak-Sliwinska et al., 2014; Ribatti, 2012).

Because treatments can be either placed onto the CAM surface or injected intravenously, there are a variety of applications for this system. For instance, the CAM assay has been extensively used to quantify angiogenesis and antiangiogenesis based on vascular density (Ribatti et al., 1997), due to the rapid growth of vasculature (Nowak-Sliwinska et al., 2014). However, this model can be limited by the presence of preexisting blood vessels (Ribatti et al., 1996; Ribatti et al., 1997; Ribatti, 2012), as, depending on the method used, it may be difficult to distinguish newly formed vasculature (Nowak-Sliwinska et al., 2014).

The ease of experimental manipulation also allows the CAM assay to be used in the investigation of tumor growth and metastasis (Herrmann et al., 2016; Ribatti, 2014), as well as to assess the efficacy of anticancer drugs (DeBord et al., 2018). Moreover, the CAM has become a useful and versatile patient-derived xenograft (PDX) platform, in which several types of tumor tissue have been grafted onto the CAM (DeBord et al., 2018) to study established and potential therapeutics and the cancer pathophysiology. The CAM assay can also be applied as an i*n vivo* model for testing materials efficacy and biocompatibility and can thus be used in the tissue engineering and regenerative medicine fields (Marshall et al., 2020; Moreno-Jiménez, et al., 2017). Finally, other applications of the CAM assay include studies of "hemodynamics, immune cell trafficking, transplantation and responses to therapy" (Nowak-Sliwinska et al., 2014).

We have previously tested whether biomaterials composed of Ubx protein genetically fused to vascular endothelial growth factor (VEGF) can promote neovascularization *in vivo* using the CAM assay (Howell et al., 2016). Fertilized eggs were cultured for 3 days continuously rotating in an egg incubator at 37 °C before being transferred to sterile cell culture dishes. After 4

days of *ex ovo* culture, EGFP-VEGF-Ubx and EGFP-Ubx fibers were placed perpendicular to established blood vessels onto the CAM. After 48 hours of materials incubation, quantification of new blood vessels resulted in an increase of 36% in neovascularization induced by EGFP-VEGF-Ubx fibers (Howell et al., 2016). Thus, to increase the angiogenic response we tested the simultaneous delivery of multiple angiogenic growth factors (GFs), including VEGF, basic fibroblast growth factor (bFGF), and stromal cell-derived factor 1α (SDF-1α), covalently incorporated into Ubx materials. Following the same protocol as previously published (Howell et al., 2016), GFs-Ubx fibers were placed on the CAM to test their ability to promote neovascularization, compared to the negative control EGFP-Ubx.

The CAM assay can be used with either *in ovo* or *ex ovo* techniques. We first used the *ex ovo* method, which consists of transferring the embryo to a sterile container (Marshall et al., 2020), such as a petri dish or a weight boat. This facilitates the visualization of embryos and allows for the application of therapeutics and test materials on the exposed CAM (Marshall et al., 2020), which is an advantage for our work since we need to quantify the formation of new blood vessels following Ubx fibers. On the other hand, our experiments were performed for a longer period of time (11 days vs average of 8 days in other studies). The longer the assay, the larger the chance that any contaminants can gain a foothold and rapidly grow, thus ruining the sample. Sources of possible contamination include the fibers, the plasticware, and, most notably, debris from the porous eggshell. Therefore, herein we describe the modified protocols that were tested in a series of attempts to reduce contamination using an assay that is well-established and has worked before. After all, we conclude that the eggshell thickness was the main problem.

3.2 Results

3.2.1 Protocol #1

To test the ability of multiple GFs incorporated into Ubx materials to stimulate neovascularization *in vivo* we used an established and reported CAM assay protocol (Howell et al., 2016), which was based on a previously published study (Bayless & Davis, 2004) (Table 1). Briefly, fertile eggs purchased from Texas A&M Poultry Science Center were incubated for 3 days at 37 °C with humidity, continuously rotating. Then the embryos were transferred to a sterile weight boat and cultured *ex ovo* for 4 days at 37 °C with humidity. Ubx fibers with or without GFs were then added on the CAM surface perpendicular to preexisting vessels. At this point, a mixture of antibiotics and antimycotics was added on the day that eggs were cracked and transferred to weight boat, and when cut, sterile western blotting filter paper wrapped with fibers were added to the embryos. As we found issues with low embryo survival rates, we hypothesized that too many antibiotics could be causing problems to the embryos and decided to only add this mix on the day of cracking the eggs into the weight boats. Thus, we changed the volume added to each egg from 600 µl to 780 µl of antibiotics and antifungal mix, based on what the final concentration should be for each one. We also decided to not use Nystatin anymore, since both Nystatin and Amphotericin B work against fungi and yeasts. The new volumes of each antibiotic and antimycotic are described in Table 2.

Although a combination of antibiotics and antimycotics was used, we still had contamination problems. To improve embryo survival rates and thus reduce contamination, we further implemented a few more modifications to our protocol to improve the sterilization of

Day 1:

1. Set up incubator. Add water to the wells and turn temperature on to 99.5 F.

Day 2:

1. Check if temperature maintained overnight.
2. Pick up eggs from Poultry Science.
3. Wash eggs with room temperature soapy water.
4. Rinse in room temperate water and place in incubator.
5. Turn on rotator. Incubate eggs for 3 days.

Day 4:

1. Autoclave gauze, metal canister top, and pre-cut blot paper.
2. Lightly spray weight boats with ethanol.
3. UV treat metal and lunch trays, weight boats and lids (overnight).

Day 5:

1. Set up hood.
    a. Clean everything out of hood
    b. Spray with ethanol
    c. Place trays in hood and arrange metal canister lid on paper towels on lunch tray
2. Stop egg rotator 30 min prior to cracking.
3. Make antibiotics (total volume for 30 eggs)
    a. 10 ml PenStrep
    b. 1 ml Gentamicin
    c. 240 µl Nystatin
    d. 100 µl Fungizone (Amphotericin B)
4. Clean eggs: remove 15 eggs from the incubator and place on egg crate. Make sure the egg's position isn't moved so that the embryo stays at the top. Wipe the eggs with betadine.
5. In the hood clean the eggs with ethanol.
6. Set up betadine bath and place first egg in.
7. Wipe excess betadine off with gauze and crack egg into weight boat. Repeat 15 times.
8. Add 600 µl of antibiotic mix to each egg and place top on.
9. Place tray in 37°C incubator. Repeat with the rest of eggs.

Day 9:

1. Wrap Ubx materials around blot paper with fibers parallel to each other.
2. Use blot paper to wipe area of CAM.
3. Place fiber on CAM with fibers perpendicular to established vessel.
4. Add 600 µl of antibiotic mix.

Day 11:

1. Take pictures of CAM and compare to pictures on Day 9.

Table 1. Protocol #1, adapted from Howell et al., 2016.

materials and tools used for this assay, which included flipping sterile weight boats and lids so that both surfaces would be sterilized by UV light and 70% EtOH spray before and after flipping the containers. However, despite of many efforts, we could not significantly reduce the chicken embryos contamination using this *ex ovo* method, and thus we decided to try a protocol reported by another laboratory.

Antibiotics and antimycotics	**Stock**	**Dilution**	**Final Concentration**	**Volume per egg**	**Volume for 30 eggs**
Gentamicin (Gibco 15710-072)	10 mg/mL	1:1000	10 µg/mL	60 µl	1.8 mL
Antibiotic/Antimycotic (Gibco 15240-062)	Penicillin 10,000 U/mL Streptomycin 10,000 µg/mL	1:100 1:100	Penicillin 100 U/mL Streptomycin 100 µg/mL	600 µl	18 mL
Amphotericin B (Sigma A2942)	250 µg/mL	1:500	0.5 µg/mL	120 µl	3.6 mL
Average volume of 60 mL per egg			Total volume of antibiotics and antimycotics	780 µl	23.4 mL

Table 2. List of antibiotics and antimycotics and their concentrations utilized in the CAM assay to reduce contamination of chicken embryos.

3.2.2 Protocol #2

In an attempt to reduce contamination of chicken embryos, we tested an *in ovo* method, in which a small window is open through the eggshell and inner shell membrane, and the embryo develops inside of the egg (Marshall et al., 2020), previously reported by a laboratory at Baylor College of Medicine (Li et al., 2015). By maintaining the shell barrier against microbes, we

hypothesized that the embryo survival rate could be increased with this method. Although the original protocol was established with specific pathogen-free embryonated eggs (Li et al., 2015) (Table 3), we still used the fertile eggs from the Poultry Science Center. In brief, eggs were incubated on rotating trays for 10 days at 36 °C and 50% humidity. On the 10th day of incubation, an egg candler was used to identify the developing embryo and the vasculature, and a sterile push pin was used to create a small hole above the air sac from which the air was removed with the help of a rubber suction bulb causing the CAM to drop away from the eggshell. Then, a Dremel rotary tool was used to create a small cut to open a window on the shell and a scotch tape was used to close the newly opened window until ready to use.

While we achieved a higher survival rate on the first test with this protocol, in which 76% of the embryos were still alive four days after windowing, we noticed that on the 10^{th} day of incubation the embryos are considerably well developed, and it was very difficult to drop the CAM away from the shell without the embryo bleeding. To fix this new problem, we adapted the protocol for our own experiments and started windowing eggs on the third day of incubation.

Although we had more success at the first try with this protocol, whenever the eggs started being manipulated to place Ubx fibers on the surface of them CAM, we would face embryos contamination again. Therefore, in another effort to improve survival rate, we tried to combine both protocols already tested to create a third, improved protocol discussed below.

Egg Incubation

1. Obtain 8-day old specific pathogen-free embryonated eggs.
2. Place eggs in rotating egg tray, stamped ends facing upwards, and place the rotating tray inside an egg incubator. Incubate eggs for 48 hr at 36 °C and 50% humidity.

Dropping the CAM and Opening the Eggs

1. Gather eggs from incubator. Place eggs in egg rack, stamped side up, and bring to laminar flow hood.
2. Turn off the room and hood lights.
3. Hold the stamped end of egg lightly to the egg candler to expose the vasculature of the CAM as well as the air sac. NOTE: The egg candler is a light source used to visualize the developing embryo and associated air sac and vasculature.
4. Place a pencil mark in between two major blood vessels.
5. Turn on the lights and use a sterile push pin to make one hole at the tip of the egg above the air sac (stamped end) and one hole at the pencil mark. Do not push the push pin all the way through; a hole around 3 mm deep will usually suffice.
6. Turn off the lights. Squeeze safety bulb, pressing the open end firmly against the hole above the air sac. Apply suction to pull air into the hole at the pencil mark, causing the CAM to drop away from the shell at the pencil mark.
7. Check that the air sac has moved from the stamped end of the egg to the pencil-marked hole using the candler. If it has not, use the push pin to make both holes slightly deeper and then re-apply suction using the safety bulb.
8. Turn on the lights. Holding the egg in one hand, turn on the Dremel rotary tool with a 15/16-inch cut-off wheel attached and make two transverse cuts just deep enough to cut through the shell but not deep enough to cut all the way down to the depressed CAM. Make the cuts around 2 cm in length and 1 cm apart from each other. Make the cuts wide enough so that a silicone ring 1 cm in diameter can pass through but thinner than the width of standard scotch tape.
9. Next, make 1 longitudinal cut between and at the ends of the two transverse cuts by lightly touching the cut-off wheel to the shell.
10. Slide sterile forceps under the shell piece and parallel to the shell. Grab the shell piece with the forceps and remove the entire piece cleanly.
11. Place scotch tape over the newly opened window, making sure to fold one end over on itself for ease of removal.
12. Place eggs back in incubator in the egg tray (NOT in the rotating egg racks) until time of inoculation.

Table 3. Protocol #2, adapted from Li et al., 2015.

3.2.3 Protocol #3

We hypothesized that a combination of sterilization steps and incubation times from Protocol #1 and the windowing method from Protocol #2 could reduce contamination and enhance survival rates before and after Ubx materials placement. Therefore, we included sterilization steps to clean the eggs before both incubation and windowing. Moreover, all of the tools and materials were very carefully sterilized with 70% ethanol, sodium hypochlorite 10% solution, and autoclave. In addition, because we also had issue with embryos not detaching from the inner membrane and shell and thus bleeding, another step was added in which we would manually rotate the eggs two or three times per day during the 5 days of incubation.

All of these modifications resulted in Protocol #3 (Table 4), which did not significantly improve the rates of embryos that either survived after windowing or after Ubx materials placement. Embryos bled because they remained attached to the shell and membrane, and high rates of contamination were still extremely challenging even after all of these protocols modifications, limiting the successful achievement our experiments.

Day 1

1. Pick up eggs from Poultry Science.
2. Clean incubator by spraying 70% Ethanol.
3. Add water to the wells and turn temperature on to ~ 25 °C.
4. Clean eggs by dipping one at a time in a container with warm betadine in the hood.
5. Let eggs air dry in the hood and place them in incubator. Turn on rotator.
6. Increase incubator temperature to 37 °C throughout the afternoon.
7. Incubate 5 days.

Day 4

1. Autoclave blades and metal to use in Dremel tool.
2. Sterilize push pins and rubber bulb with 10% bleach solution for 30 minutes, rinse a few times with sterile water, then soak in 70% ethanol for another 30 minutes.
3. Wipe hood with 70% ethanol and let materials dry in the hood.

Day 5

1. Set up hood
    a. Clean everything out of hood.
    b. Wipe hood with germicidal wipes.
    c. Spray with 70% ethanol inside and outside of hood, including the light and electricity buttons.
2. Gather 7 eggs from incubator, place them in egg rack, and bring to hood. Turn off the room and hood lights.
3. Wipe the eggshell with paper towel and 70% ethanol. Hold the round end of egg lightly to the egg candler to expose the vasculature of the CAM as well as the air sac.
4. Use a sharpie pencil to mark in between two major blood vessels and air sac.
5. Turn on the lights and use a sterile push pin to make one hole on the air sac and one hole at the pencil mark on top – make sure to not reach any blood vessel.
6. Using sterile push pin should be enough to move the air sac to the top and make the CAM to drop away from the shell. If not, use bulb, pressing the open end firmly against the hole on the air sac. Apply suction to pull air out of the hole at the pencil mark, causing the CAM to drop away from the shell at the pencil mark.
7. Check that the air sac has moved from the round end of the egg to the pencil-marked hole on top using the candler. If it has not, use the push pin to make both holes slightly deeper and then re-apply suction using the safety bulb.
8. Turn on the hood lights. Holding the egg in one hand, turn on the Dremel rotary tool with a 15/16-inch cut-off wheel attached and make two transverse cuts just deep enough to cut through the shell but not deep enough to cut all the way down to the depressed CAM. Make the cuts around 2 cm in length and 1 cm apart from each other. Make the cuts wide enough so that thin blot paper or inoculation loop wrapped with materials can pass through but thinner than the width of standard scotch tape.
9. Next, make 1 longitudinal cut between and at the ends of the two transverse cuts by lightly touching the cut-off wheel to the shell.
10. Slide sterile forceps under the shell piece and parallel to the shell. Grab the shell piece with the forceps and remove the entire piece cleanly.

Table 4. Protocol #3, adapted from previous protocols #1 and #2.

Table 4 Continued

11. Place scotch tape over the newly opened window, making sure to fold one end over on itself for ease of removal.
12. Place eggs in incubator in tissue culture room until Day 7. Make sure to add sterile water to the tray in the incubator to keep it humid.

Day 7

1. Autoclave forceps and pre-cut blot paper.
2. Wrap Ubx materials around blot paper with fibers parallel to each other.
3. Use Q-tips wet in autoclaved PBS to wipe area of CAM.
4. Place materials on CAM with fibers perpendicular to established vessel.
5. Take pictures of CAMs.

Day 9

Take pictures of CAMs and compare to pictures on Day 7.

3.2.4 Protocol #4

In a last attempt to perform the CAM assay, we hypothesized that using a Dremel rotary tool to cut windows open could be the source of contamination, as this tool creates a lot of eggshell dust. Although the eggshell may function as a barrier against microorganisms, it is extremely porous and thus could also be the cause of embryos contamination. Therefore, I tried a new protocol in which windows are open on the eggshell using scissors (Table 5) (Korn & Cramer, 2007). Briefly, a piece of stretchy, plastic tape is placed on the base of the egg and about 4 mL of albumen is aspirated using a syringe with an 18-gauge needle, so that the embryo drops away from the shell. Then, another piece of tape is placed on top of the egg and a window is cut open with scissors.

I first practiced this method with 36 groceries eggs, and it worked well. Then we ordered another batch of 30 fertile eggs from Poultry Science Center for the real experiment and found problems such as eggshell cracking before windowing, or embryos bleeding because the CAM

did not drop away from the shell. I was able to open windows in 8 of the 30 eggs, but they were all contaminated and some had leaked on the next day. We concluded that the eggshells were too fragile for this approach to succeed.

3.3 Conclusions

While testing different protocols, we were able to reduce contamination and improve chicken embryo survival rates to some extent, as summarized in Table 6. However, those rates were not sufficient to achieve a significant sample size and to complete the whole experiment, which included keeping the embryos alive and growing for a period of almost 10 days, placing Ubx materials on the CAM surface, and, finally, quantifying the formation of new blood vessels after 48 hours of incubation with Ubx fibers.

Each protocol of CAM assay tested herein had its difficulties and required adaptations to work. For instance, cracking the eggs into sterile weight boats with metal canister was difficult because the egg yolk can be easily damaged. Moreover, although we have reduced the period of incubation before starting our experiments to avoid embryos bleeding, some embryos were attached to the eggshell or inner membrane and would not drop away. While a study reported high embryo survival rate, easy methodology, and sterility not required as advantages of the CAM assay (Ribatti, 2012), these topics were limitations to our work.

Overall, I believe that Protocol #4 offers an easier way to open windows on the eggshell without the need of a harsh tool. The size of the windows can also be somewhat controlled, which facilitates the visualization of blood vessels and placement of Ubx materials. Finally, we

conclude that the eggshell of fertile eggs from our source could not handle our experiments, and thus we focused on stimulating neovascularization with Ubx materials using a mouse model.

Remove eggs from incubator

1. Maintain at 37°C with relative humidity set above 60%.
2. Remove the eggs; turn eggs 90° so that the large base lies horizontal.

Swab eggs to sterilize

1. Saturate a stack of non-sterile gauze with 70% ethanol.
2. Use two to three pieces to swab up to 5 eggs. Discard when the gauze is soiled.

Preparing albumen removal site

1. Cut and place a 1" x 1" piece of 3M plastic tape just left of the base to protect the area where the albumin will be drawn out.

Removal of albumen

1. Use the point of a pair of scissors to make a small hole in the middle of the tape.
2. Using a 10-cc syringe with an 18-gauge, 1-inch needle, slowly drill the needle through the hole made by the scissors.
3. Drive the needle down at a 45°C angle towards the bottom of the egg.
4. Tilt the needle towards the center and draw up 3 to 4 mL of albumen.

Windowing

1. Cut a 3" x 3" piece of plastic tape and stretch it to fit on the top of the egg. Extend the corners of the square around the rounded ends of the horizontal surface of the eggs, being careful not to pull too hard. Pull the tape so that it is tight against the surface of the eggs with no folds.
2. Using a pair of sharp-straight 4" dissection scissors, twist a hole into the bottom center of the area where the tape was placed. Slowly guide the lower blade of the scissors into the egg being sure to keep the tips up against the inside of the shell. Direct the blade towards the base and slowly begin to cut the shell. Proceed in a counterclockwise fashion, stopping just before reaching the top center. Remove the scissors and repeat going in the opposite direction until only a small bit of the egg remains attached. Check to be sure the egg is fertilized. Shut the window.

Closing, reopening and sealing the egg

1. Cut about a 2-3" long by 1/2" wide plastic tape and shut the window so it fits back into the hole that was cut. Take another 1 x 1" piece of tape and seal the hole from which the egg was drained. Use a pair of forceps to reopen the egg to do any manipulations. When you're ready to return the eggs to the incubator, cut a piece of tape that is large enough to seal the window and cover the entire horizontal surface of the egg.

Table 5. Protocol #4, adapted from Korn & Cramer, 2007.

Protocol	Number of eggs tested	% Eggs survived before materials	% Eggs survived after materials	% Eggs dead
#1	219	29.10	36	88.1
#2	245	35.9	68.3	77.4
#3	72	43.2	52.9	77.2
#4	8	0	0	100

Table 6. Summary of the different CAM assay protocols that were tested and the modifications that were made to improve chicken embryo survival rate and to reduce contamination.

The number of eggs tested for each protocol includes non-fertile/groceries eggs used for practice, the eggs tested with the original protocol, and the eggs tested with modifications in the protocol. The other 3 columns represent the number of fertile eggs used for the assays with Ubx materials, with or without modifications in protocols.

CHAPTER IV

CONCLUSIONS AND FUTURE DIRECTIONS

4.1 Conclusions

Each protein-based material has a unique set of characteristics that define its optimal applications, such as biocompatibility, surface chemistry, and mechanical properties. Applying the protein fusion technique allows creation of covalently functionalized materials in a single pot, single component, single step reaction. For each self-assembling protein, the design of protein fusions will be limited by factors such as protein size, stability, and fusion order, that are unique for that material. Nevertheless, the number of materials that have been functionalized by protein fusion has expanded in the last decade, creating new opportunities for materials engineering and functionalization. The size and complexity of functional proteins that can be incorporated by protein fusion have also increased dramatically.

Many applications may require the functional proteins to be patterned within the materials. For instance, tissues are composed of many cell types, and thus the proteins that instruct each cell type, as well as the target cells, will ultimately have to be entrapped within the material. Developing more general and more versatile techniques for patterning proteins would significantly expand the number of protein materials that could be used in applications requiring this approach. Additionally, applications may require functionalized protein-based materials to interface with other types of materials. In tissue engineering, interfaces between tissue types (e.g., bone/tendon) may be required to rebuild damaged bodies. Likewise, sensors must not only

bind ligand, but also detect when ligand is present. New proteins may need to be designed or evolved to meet these needs.

Addressing these issues will substantially increase the utility of all protein-based materials. In addition, each protein-based material exhibits a unique set of beneficial attributes and engineering challenges. Identifying new self-assembling proteins amenable to protein fusion and defining the range of proteins that can be successfully fused will expand the toolbox, allowing materials to be selected that better match the needs of each application. Finally, developing creative assembly techniques may help incorporate difficult proteins that cannot be immobilized by standard single-component approaches.

4.2 Future directions for Ubx materials and multiple growth factors

A broad range of proteins of varying sizes, charges, and quaternary structures have already been successfully incorporated into Ubx materials. This dissertation demonstrates how multiple pro-angiogenic GFs maintained their activity once immobilized in these materials, despite their different three-dimensional structures.

As part of this dissertation, I had to solve many technical problems: how to design constructs that would not significantly impact materials assembly, how to stabilize growth factors and prevent degradation, how to handle and store the materials, how to keep Ubx fibers with microscale diameters sterile and intact during cell culture, on chicken embryos, and in mice wounds. Thus, additional applications for growth factors fused to Ubx materials are expected to have lower difficulty.

The mechanical properties, biocompatibility, and biodegradability of Ubx materials are advantageous for numerous biomedical applications. In addition, as discussed previously, stimulation and formation of new blood vessels is also necessary for many important applications, such as tissue engineering and regenerative medicine. Ubx materials are also compatible with different cell types and thus other proteins could be incorporated to direct cell behavior for specific applications. A few potential applications that would benefit from Ubx materials displaying growth factors and modulating cell response are described below.

Wound healing is a complex process that involves growth factors, chemokines, and other biomolecules. Studies have shown that specific growth factors and cytokines play a role in healing and their topical administration enhances wound closure (Nurkesh et al., 2020). Therefore, many strategies rely on delivery of GFs involved in wound healing to accelerate the process of tissue regeneration. However, the direct application of GFs alone is difficult due to poor skin penetration, loss of activity of GFs, the need for prolonged delivery of GFs for wound healing and repetitive doses may result in adverse side effects such as cancer (Nurkesh et al., 2020), among other challenges.

Incorporating these growth factors into Ubx materials via protein fusion has the potential to solve these problems, as demonstrated previously in Chapter II. Because different ratios of growth factors can be used, new combinations can accommodate more growth factors. Additionally, antimicrobial peptides can also be genetically fused to Ubx to stimulate the proliferation and growth of different cell types, i.e., fibroblasts, epithelial, and immune cells, and thus support enhanced wound healing (Lei et al., 2019; Taniguchi et al., 2019).

Bioengineered tissues require extensive vascularization prior to implantation into the patient. Lack of or insufficient vascularization is one of the major limitations in vascular tissue engineering and may cause poor tissue integration and cell death (Rouwkema & Khademhosseini, 2016). The need to provide cells with oxygen and nutrients and thus promote rapid integration of bioengineered constructs with host vasculature drives the development of prevascularized engineered tissues (Rouwkema & Khademhosseini, 2016).

A potential strategy to use Ubx materials in this specific application is to seed endothelial cells onto Ubx fibers displaying growth factors prior to implantation to promote EC migration, survival and proliferation on collagen 3D matrices. Additionally, co-culture with other cell types, such as fibroblasts and endothelial progenitor cells (EPCs), in appropriate culture conditions can promote the formation of vascular networks for prevascularization of scaffolds (Chandra & Atala, 2019; Song et al., 2018). This approach could potentially enhance blood flow and viability of constructs following implantation into animal models.

Ubx materials can also be functionalized with other growth factors that play important roles in neovascularization and wound healing. For instance, platelet-derived growth factor (PDGF-BB) and hepatocyte growth factor (HGF) have already been fused to Ubx. However, these protein fusions were inserted into constructs that could prevent materials assembly or growth factor activity. This problem could be solved by inserting the growth factors' DNA sequences into a more recently designed construct, which has already been used for double fusions of EGFP and each of the growth factors studied in Chapter II and does not impact materials formation and activity.

For proof-of-concept purposes, Ubx fibers manually wrapped around sterile, plastic inoculation loops could be tested, similarly to the methods developed for this dissertation. It would be possible to wrap Ubx fibers directly on the collagen matrices depending on their stiffness. Ideally, for a higher scale production, electrospun Ubx fibers with growth factors and other proteins or peptides should be used.

Growth factors are also utilized as therapeutic strategies to treat peripheral nerve injury (PNI). Examples of GFs involved in the development and regeneration of the nervous system include nerve growth factor (NGF), brain-derived neurotrophic factor (BDNF), FGF, and insulin-like growth factor (IGF) (R Li et al., 2020; Zhang et al., 2019). Similar to neovascularization, the simultaneous delivery of a combination of growth factors is advantageous and may result in a synergistic effect on accelerating nerve regeneration (Chen et al., 2010; R Li et al., 2020). Therefore, Ubx materials can possibly be an approach to display growth factors for the treatment of PNI.

4.3 Other potential applications of Ubx materials: hydrogels

Hydrogels are biomaterials comprised of 3D polymeric networks that form a porous structure though either physical or chemical crosslinking and can hold a large amount of water (Ahn et al., 2021; Katyal et al., 2020). Protein-based hydrogels are biocompatible, biodegradable, and have tunable properties (Ahn et al., 2021). Examples of naturally self-assembling proteins that can be used to create hydrogels include silk, elastin, collagen, and resilin (Ahn et al., 2021). There is a wide variety of biomedical applications for hydrogels, such as cell encapsulation, drug delivery, cancer therapy, bioprinting, biosensors, and tissue

engineering (Łabowska et al., 2021; Ahn et al., 2021; Bastiancich et al., 2016; Herrmann et al., 2021; Seliktar, 2012).

We have previously attempted to create thermally responsive hydrogels made of Ubx protein chemically crosslinked with glutaraldehyde or enzymatically crosslinked with horseradish peroxidase (HRP) and hydrogen peroxide (H_2O_2), among others (Aeschbach et al., 1976; Bigi et al., 2001; Bigi et al., 2002). The goal was to fuse anti-cancer drugs to Ubx and create injectable Ubx hydrogels that would solidify at body temperature (~ 37 ºC) for localized cancer therapy (Bastiancich et al., 2016). However, these hydrogels either failed to solidify or could not maintain their solid state for more than a few minutes. For proof-of-concept purposes, Ubx hydrogels could be tested with higher concentrations of crosslinkers reported by other studies (Chen et al., 2013; Jackson et al., 2021; Khanmohammadi et al., 2018). While these are a few options, there are many other possibilities to crosslink Ubx to create hydrogels.

Another potential application for Ubx hydrogels would be 3D vascularization. In this scenario, Ubx hydrogels displaying growth factors could be used as a platform to attract cells, stimulate their survival and proliferation, and promote the formation of 3D tubule-like structures. These structures could be implanted for tissue engineering and regenerative medicine applications, such as wound treatment. Similarly, an injectable Ubx hydrogel for sustained delivery of therapeutic growth factors could be tested for diabetic foot ulcers or cutaneous wound injury.

Alternatively, Ubx-based hydrogels would find application in 3D *in vitro* cell culture to deliver molecules to direct cell behavior. Because we can incorporate growth factors into Ubx materials, a 3D model of tumor vascularization could be created with Ubx hydrogels, in which co-culture of different cell lines, growth factors, and other chemical cues present at the tumor microenvironment could be replicated *in vitro*. Finally, the use of Ubx hydrogels as inks for 3D printing could also be explored in the future.

REFERENCES

Łabowska, M., Cierlukm, K., Jankowska, A., Kulbacka, J., Detyna, J., & Michalak, I. (2021). A Review on the Adaption of Alginate-Gelatin Hydrogels for 3D Cultures and Bioprinting. *Materials (Basel), 14*(4), 858. doi: 10.3390/ma14040858.

Abbas, M., Zou, Q., Li, S., & Yan, X. (2017). Self-assembled peptide- and protein-based nanomaterials for antitumor photodynamic and photothermal therapy. *Advanced Materials, 29*(12), 1605021. doi: 10.1002/adma.201605021.

Adams, R. H., & Alitalo, K. (2007). Molecular regulation of angiogenesis and lymphangiogenesis. *Nature Reviews Molecular Cell Biology, 8*(6), 464-478. doi: 10.1038/nrm2183.

Aeschbach, R., Amadò, R., & Neukom, H. (1976). Formation of dityrosine cross-links in proteins by oxidation of tyrosine residues. *Biochimica et Biophysica Acta, 439*(2), 292-301. doi: 10.1016/0005-2795(76)90064-7.

Ahn, W., Lee, J. H., Kim, S. R., Lee, J., & Lee, E. J. (2021). Designed protein- and peptide-based hydrogels for biomedical sciences. *Journal of Materials Chemistry B, 9*(8), 1919-1940. doi: 10.1039/d0tb02604b.

An, B., DesRochers, T. M., Qin, G., Xia, X., Thigarajan, G., Brodsky, B., & Kaplan, D. L. (2013). The influence of specific binding of collagen-silk chimeras to silk biomaterials on hMSC behavior. *Biomaterials, 43*(2), 402–412. doi: 10.1016/j.biomaterials.2012.09.085.

Atienza-Roca, P., Cui, X., Hooper, G., Woodfield, T., & Lim, K. (2018). Growth Factor Delivery Systems for Tissue Engineering and Regenerative Medicine. *Advances in Experimental Medicine and Biology, 1078*, 245-269. doi: 10.1007/978-981-13-0950-2_13.

Auerbach, R., Kubai, L., Knighton, D., & Folkman, J. (1974). A simple procedure for the long-term cultivation of chicken embryos. *Developmental Biology, 41*(2), 391-394. doi: 10.1016/0012-1606(74)90316-9.

Augustine, R., Prasad, P., & Khalaf, I. M. (2019). Therapeutic angiogenesis: From conventional approaches to recent nanotechnology-based interventions. *Materials Science & Engineering. C, Materials for Biological Applications, 97*, 994-1008. doi: 10.1016/j.msec.2019.01.006.

Ausprunk, D. H., Knighton, D. R., & Folkman, J. (1974). Differentiation of vascular endothelium in the chick chorioallantois: a structural and autoradiographic study. *Developmental Biology, 38*(2), 237-248. doi: 10.1016/0012-1606(74)90004-9.

Bai, Y., Bai, L., Zhou, J., Chen, H., & Zhang, L. (2018). Sequential delivery of VEGF, FGF-2 and PDGF from the polymeric system enhance HUVECs angiogenesis in vitro and CAM angiogenesis. *Cellular Immunology, 323*, 19-32. doi: 10.1016/j.cellimm.2017.10.008.

Bai, Y., Lee, P. F., Gibbs, H. C., Bayless, K. J., & Yeh, A. T. (2014). Dynamic multicomponent engineered tissue reorganization and matrix deposition measured with an integrated nonlinear optical microscopy-optical

coherence microscopy system. *Journal of Biomedical Optics, 19*(3), 36014. doi: 10.1117/1.JBO.19.3.036014.

Baiguera, S., & Ribatti, D. (2013). Endothelialization approaches for viable engineered tissues. *Angiogenesis, 8*(3), 1-14. doi: 10.1007/s10456-012-9307-8.

Bastiancich, C., Danhier, P., Préat, V., & Danhier, F. (2016). Anticancer drug-loaded hydrogels as drug delivery systems for the local treatment of glioblastoma. *Journal of Controlled Release, 243*, 29-42. doi: 10.1016/j.jconrel.2016.09.034.

Bax, D. V., Smalley, H. E., Farndale, R. W., Best, S. M., & Cameron, R. E. (2019). Cellular response to collagen-elastin composite materials. *Acta Biomaterialia, 86*, 158-170. doi: 10.1016/j.actbio.2018.12.033.

Bayless, K. J., & Davis, G. E. (2004). Microtubule depolymerization rapidly collapses capillary tube networks in vitro and angiogenic vessels in vivo through the small GTPase Rho. *Journal of Biological Chemistry, 279*(12), 11686-11695. doi: 10.1074/jbc.M308373200.

Bayless, K. J., Kwak, H. I., & Su, S. C. (2009). Investigating endothelial invasion and sprouting behavior in three-dimensional collagen matrices. *Nature Protocols, 4*, 1888-1898. doi: 10.1038/nprot.2009.221.

Bellas, E., Lo, T. J., Fournier, E. P., Brown, J. E., Abbott, R. D., Gil, E. S., . . . Kaplan, D. L. (2015). Injectable silk foams for soft tissue regeneration.

Advanced Healthcare Materials, 4(3), 452–459. doi: 10.1002/adhm.201400506.

Bigi, A., Cojazzi, G., Panzavolta, S., Roveri, N., & Rubini, K. (2002). Stabilization of gelatin films by crosslinking with genipin. *Biomaterials, 23*(24), 4827-4832. doi: 10.1016/s0142-9612(02)00235-1.

Bigi, A., Cojazzi, G., Panzavolta, S., Rubini, K., & Roveri, N. (2001). Mechanical and thermal properties of gelatin films at different degrees of glutaraldehyde crosslinking. *Biomaterials, 22*(8), 763-768. doi: 10.1016/s0142-9612(00)00236-2.

Borgo, B., & Havranek, J. J. (2012). Automated selection of stabilizing mutations in designed and natural proteins. *Proceedings of the National Academy of Sciences of the United States of America , 109*(5), 1494-1499. doi: 10.1073/pnas.1115172109.

Bracalello, A., Santopietro, V., Vassalli, M., Marletta, G., Del Gaudio, R., Bochicchio, B., & Pepe, A. (2011). Design and production of a chimeric resilin-, elastin-, and collagen-like engineered polypeptide. *Biomacromolecules, 12*(8), 2957–2965. doi: 10.1021/bm2005388.

Brudno, Y., Ennett-Shepard, A. B., Chen, R. R., Aizenberg, M., & Mooney, D. J. (2013). Enhancing microvascular formation and vessel maturation through temporal control over multiple pro-angiogenic and pro-maturation factors. *Biomaterials, 34*(36), 9201-9209. doi: 10.1016/j.biomaterials.2013.08.007.

Cao, J., Wang, P., Liu, Y., Zhu, C., & Fan, D. (2020). Double crosslinked HLC-CCS hydrogel tissue engineering scaffold for skin wound healing. *International Journal of Biological Macromolecules, 155*, 625–635. doi: 10.1016/j.ijbiomac.2020.03.236.

Cao, L., & Mooney, D. J. (2007). Spatiotemporal control over growth factor signaling for therapeutic neovascularization. *Advanced Drug Delivery Reviews, 59*(13), 1340-1350. doi: 10.1016/j.addr.2007.08.012.

Carmeliet, P. (2000). Mechanisms of angiogenesis and arteriogenesis. *Nature Medicine, 6*(4), 389-395. doi: 10.1038/74651.

Carmeliet, P., & Jain, R. K. (2000). Angiogenesis in cancer and other diseases. *Nature, 407*(6801), 249-257. doi: 10.1038/35025220.

Carmeliet, P., & Jain, R. K. (2011). Molecular mechanisms and clinical applications of angiogenesis. *Nature, 473*(7347), 298-307. doi: 10.1038/nature10144.

Carragee, E., Chu, G., Rohatgi, R., Hurwitz, E., Weiner, B. K., Yoon, S. T., . . . Kopjar, B. (2013). Cancer risk after use of recombinant bone morphogenetic protein-2 for spinal arthrodesis. *The Journal of Bone and Joint Surgery, 95*(17), 1537–1545. doi: 10.2106/JBJS.L.01483.

Chandra, P., & Atala, A. (2019). Engineering blood vessels and vascularized tissues: technology trends and potential clinical applications. *Clinical Science, 133*(9), 1115-1135. doi: 10.1042/CS20180155.

Chen, F. M., Zhang, M., & Wu, Z. F. (2010). Toward delivery of multiple growth factors in tissue engineering. *Biomaterials, 31*(24), 6279-6308. doi: 10.1016/j.biomaterials.2010.04.053.

Chen, P. Y., Dang, X., Klug, M. T., Qi, J., Dorval Courchesne, N. M., Burpo, F. J., . . . Belcher, A. M. (2013). Versatile three-dimensional virus-based template for dye-sensitized solar cells with improved electron transport and light harvesting. *ACS Nano, 7*(8), 6563-6574. doi: 10.1021/nn4014164.

Chiu, L. L., & Radisic, M. (2010). Scaffolds with covalently immobilized VEGF and Angiopoietin-1 for vascularization of engineered tissues. *Biomaterials, 31*(2), 226-241. doi: 10.1016/j.biomaterials.2009.09.039.

Da Costa, A., Pereira, A. M., Gomes, A. C., Rodriguez-Cabello, J. C., Sencadas, V., Casal, M., & Machado, R. (2017). Single step fabrication of antimicrobial fibre mats from a bioengineered protein-based polymer. *Biomedical Materials, 12*(4), 045011. doi: 10.1088/1748-605X/aa7104.

Dean, S. N., Turner, K. B., Medintz, I. L., & Walper, S. A. (2017). Targeting and delivery of therapeutic enzymes. *Therapeutic Delivery, 8*(7), 577-595. doi: 10.4155/tde-2017-0020.

DeBord, L. C., Pathak, R. R., Villaneuva, M., Liu, H. C., Harrington, D. A., Yu, W., . . . Sikora, A. G. (2018). The chick chorioallantoic membrane (CAM) as a versatile patient-derived xenograft (PDX) platform for precision

medicine and preclinical research. *American Journal of Cancer Research, 8*(8), 1642-1660.

DeLong, S. A., Moon, J. J., & West, J. L. (2005). Covalently immobilized gradients of bFGF on hydrogel scaffolds for directed cell migration. *Biomaterials, 26*(16), 3227-3234. doi: 10.1016/j.biomaterials.2004.09.021.

Demidova-Rice, T. N., Durham, J. T., & Herman, I. M. (2012). Wound Healing Angiogenesis: Innovations and Challenges in Acute and Chronic Wound Healing. *Advances in Wound Care, 1*(1), 17-22. doi: 10.1089/wound.2011.0308.

Dinjaski, N., Plowright, R., Zhou, S., Belton, D. J., Perry, C. C., & Kaplan, D. L. (2017). Osteoinductive recombinant silk fusion proteins for bone regeneration. *Acta Biomaterialia, 49*, 127–139. doi: 10.1016/j.actbio.2016.12.002.

Doblhofer, E., & Scheibel, T. (2015). Engineering of recombinant spider silk proteins allows defined uptake and release of substances. *Journal of Pharmaceutical Sciences, 104*(3), 988–994. doi: 10.1002/jps.24300.

Dor, Y., Djonov, V., Abramovitch, R., Itin, A., Fishman, G. I., Carmeliet, P., . . . Keshet, E. (2002). Conditional switching of VEGF provides new insights into adult neovascularization and pro-angiogenic therapy. *The EMBO Journal, 21*(8), 1939-1947. doi: 10.1093/emboj/21.8.1939.

Duran, C. L., Howell, D. W., Dave, J. M., Smith, R. L., Torrie, M. E., Essner, J. J., & Bayless, K. J. (2017). Molecular Regulation of Sprouting

Angiogenesis. *Comprehensive Physiology, 8*(1), 153-235. doi: 10.1002/cphy.c160048.

Dvorak, H. F., Brown, L. F., Detmar, M., & Dvorak, A. M. (1995). Vascular permeability factor/vascular endothelial growth factor, microvascular hyperpermeability, and angiogenesis. *The American Journal of Pathology, 146*(5), 1029-1039.

Filipowska, J., Tomaszewski, K. A., Niedźwiedzki, Ł., Walocha, J. A., & Niedźwiedzki, T. (2017). The role of vasculature in bone development, regeneration and proper systemic functioning. *Angiogenesis, 20*(3), 291-302. doi: 10.1007/s10456-017-9541-1.

Güler, R., Thatikonda, N., Ghani, H. A., Hedhammar, M., & Löfblom, J. (2019). VEGFR2-Specific Ligands Based on Affibody Molecules Demonstrate Agonistic Effects when Tetrameric in the Soluble Form or Immobilized via Spider Silk. *ACS Biomaterials Science & Engineering, 5*(12), 6474-6484. doi: 10.1021/acsbiomaterials.9b00994.

Gianni-Barrera, R., Di Maggio, N., Melly, L., Burger, M. G., Mujagic, E., Gürke, L., . . . Banfi, A. (2020). Therapeutic vascularization in regenerative medicine. *Stem Cells Translational Medicine, 9*(4), 433-444. doi: 10.1002/sctm.19-0319.

Girotti, A., Orbanic, D., Ibáñez-Fonseca, A., Gonzalez-Obeso, C., & Rodríguez-Cabello, J. C. (2015). Recombinant technology in the development of

materials and systems for soft-tissue repair. *Advanced Healthcare Materials, 4*(16), 2423–2455. doi: 10.1002/adhm.201500152.

Glasscock, C. J., Lucks, J. B., & DeLisa, M. P. (2016). Engineered protein machines: Emergent tools for synthetic biology. *Cell Chemical Biology, 23*(1), 45-56. doi: 10.1016/j.chembiol.2015.12.004.

Gomes, S., Leonor, I. B., Mano, J. F., Reis, R. L., & Kaplan, D. L. (2011). Spider silk-bone sialoprotein fusion proteins for bone tissue engineering. *Soft Matter, 7*(10), 4964-4973. doi: 10.1039/C1SM05024A.

Gomes, S., Leonor, I. B., Mano, J. F., Reis, R. L., & Kaplan, D. L. (2012). Natural and Genetically Engineered Proteins for Tissue Engineering. *Progress in Polymer Science, 37*(1), 1–17. doi: 10.1016/j.progpolymsci.2011.07.003.

Goor, O. J., Hendrikse, S. I., Dankers, P. Y., & Meijer, E. W. (2017). From supramolecular polymers to multi-component biomaterials. *Chemical Society Reviews, 46*(21), 6621-6637. doi: 10.1039/c7cs00564d.

Gray, B. P., & Brown, K. C. (2014). Combinatorial peptide libraries: Mining for cell-binding peptides. *Chemical Reviews, 114*(2), 1020-1081. doi: 10.1021/cr400166n.

Greer, A. M., Huang, Z., Oriakhi, A., Lu, Y., Lou, J., Matthews, K. S., & Bondos, S. E. (2009). The Drosophila transcription factor ultrabithorax self-assembles into protein-based biomaterials with multiple morphologies. *Biomacromolecules, 10*(4), 829-837. doi: 10.1021/bm801315v.

Grieshaber, S. E., Farran, A. J., Bai, S., Kiick, K. L., & Jia, X. (2012). Tuning the properties of elastin mimetic hybrid copolymers via a modular polymerization method. *Biomacromolecules, 13*(6), 1774–1786. doi: 10.1021/bm3002705.

Grieshaber, S. E., Farran, A. J., Lin-Gibson, S., Kiick, K. L., & Jia, X. (2009). Synthesis and characterization of elastin-mimetic hybrid polymers with multiblock, alternating molecular architecture and elastomeric properties. *Macromolecules, 42*(7), 2532–2541. doi: 10.1021/ma802791z.

Herbert, S. P., & Stainier, D. Y. (2011). Molecular control of endothelial cell behaviour during blood vessel morphogenesis. *Nature Reviews Molecular Cell Biology, 12*(9), 551-564. doi: 10.1038/nrm3176.

Herrmann, A., Haag, R., & Schedler, U. (2021). Hydrogels and Their Role in Biosensing Applications. *Advanced Healthcare Materials, 10*(11), e2100062. doi: 10.1002/adhm.202100062.

Herrmann, A., Moss, D., & Sée, V. (2016). The Chorioallantoic Membrane of the Chick Embryo to Assess Tumor Formation and Metastasis. *Methods in Molecular Biology, 1464*, 97-105. doi: 10.1007/978-1-4939-3999-2_9.

Hollingshead, S., Lin, C. Y., & Liu, J. C. (2017). Designing smart materials with recombinant proteins. *Macromolecular Bioscience, 17*(7), 1600554. doi: 10.1002/mabi.201600554.

Horak, J., Jansson, R., Dev, A., Nilebäck, L., Behnam, K., Linnros, J., . . . Karlström, A. E. (2018). Recombinant spider silk as mediator for one-step,

chemical-free surface biofunctionalization. *Advanced Functional Materials, 28*(21), 1800206. doi: 10.1002/adfm.201800206.

Hou, L., Kim, J. J., Woo, Y. J., & Huang, N. F. (2016). Stem cell-based therapies to promote angiogenesis in ischemic cardiovascular disease. *American Journal of Physiology. Heart and Circulatory Physiology, 310*(4), H455-465. doi: 10.1152/ajpheart.00726.2015.

Howell, D. W., Duran, C. L., Tsai, S.-P., Bondos, S. E., & Bayless, K. J. (2016). Functionalization of Ultrabithorax materials with vascular endothelial growth factor enhances angiogenic activity. *Biomacromolecules, 17*(11), 3558−3569. doi: 10.1021/acs.biomac.6b01068.

Howell, D. W., Tsai, S. P., Churion, K., Patterson, J., Abbey, C., Atkinson, J. T., . . . Bondos, S. E. (2015). Identification of multiple dityrosine bonds in materials composed of the Drosophila protein Ultrabithorax. *Advanced Functional Materials, 25*(37), 5988-5998. doi: 10.1002/adfm.201502852.

Hu, X., Cebe, P., Weiss, A. S., Omenetto, F., & Kaplan, D. L. (2012). Protein-based composite materials. *Materials Today, 15*(5), 208-215. doi: 10.1016/S1369-7021(12)70091-3.

Hu, X., Xia, X. X., Huang, S. C., & Qian, Z. G. (2019). Development of Adhesive and Conductive Resilin-Based Hydrogels for Wearable Sensors. *Biomacromolecules, 20*(9), 3283-3293. doi: 10.1021/acs.biomac.9b00389.

Huang, W., Rollett, A., & Kaplan, D. L. (2015). Silk-elastin-like protein biomaterials for the controlled delivery of therapeutics. *Expert Opinion on Drug Delivery, 12*(5), 779–791. doi: 10.1517/17425247.2015.989830.

Huang, Z., Lu, Y., Majithia, R., Shah, J., Meissner, K., Matthews, K. S., . . . Lou, J. (2010). Size dictates mechanical properties for protein fibers self-assembled by the Drosophila hox transcription factor ultrabithorax. *Biomacromolecules, 11*(12), 3644-3651. doi: 10.1021/bm1010992.

Huang, Z., Salim, T., Brawley, A., Patterson, J., Matthews, K. S., & Bondos, S. E. (2011). Functionalization and patterning of protein-based materials using active ultrabithorax chimeras. *Advanced Functional Materials*, *21*(14), 2633−2640. doi: 10.1002/adfm.201100067.

Isaacson, K. J., Jensen, M. M., Watanabe, A. H., Green, B. E., Correa, M. A., Cappello, J., & Ghandehari, H. (2018). Self-assembly of thermoresponsive recombinant silk-elastinlike nanogels. *Macromolecular Bioscience, 18*(1), 1700192. doi: 10.1002/mabi.201700192.

Izadifar, M., Kelly, M. E., & Chen, X. (2016). Regulation of sequential release of growth factors using bilayer polymeric nanoparticles for cardiac tissue engineering. *Nanomedicine (London, England), 11*(24), 3237-3259. doi: 10.2217/nnm-2016-0220.

Jackson, K., Peivandi, A., Fogal, M., Tian, L., & Hosseinidoust, Z. (2021). Filamentous Phages as Building Blocks for Bioactive Hydrogel. *ACS Applied Bio Materials, 4*(3), 2262–2273. doi: 10.1021/acsabm.0c01557.

Jahani, M., Rezazadeh, D., Mohammadi, P., Abdolmaleki, A., Norooznezhad, A., & Mansouri, K. (2020). Regenerative Medicine and Angiogenesis; Challenges and Opportunities. *Advanced Pharmaceutical Bulletin, 10*(4), 490-501. doi: 10.34172/apb.2020.061.

Jain, R. K. (2003). Molecular regulation of vessel maturation. *Nature Medicine, 9*(6), 685–693. doi: 10.1038/nm0603-685.

Jain, R. K., Au, P., Tam, J., Duda, D. G., & Fukumura, D. (2005). Engineering vascularized tissue. *Nature Biotechnology, 23*(7), 821-823. doi: 10.1038/nbt0705-821.

Jansson, R., Courtin, C. M., Sandgren, M., & Hedhammar, M. (2015). Rational design of spider silk materials genetically fused with an enzyme. *Advanced Functional Materials, 25*(33), 5343-5352. doi: 10.1002/adfm.201501833.

Jansson, R., Thatikonda, N., Lindberg, D., Rising, A., Johansson, J., Nygren, P. A., & Hedhammar, M. (2014). Recombinant spider silk genetically functionalized with affinity domains. *Biomacromolecules, 15*(5), 1696-1706. doi: 10.1021/bm500114e.

Jia, F., Narasimhan, B., & Mallapragada, S. (2014). Materials-based strategies for multi-enzyme immobilization and co-localization: A review. *Biotechnology and Bioengineering, 111*(2), 209-222. doi: 10.1002/bit.25136.

Kant, R. J., & Coulombe, K. L. (2018). Integrated approaches to spatiotemporally directing angiogenesis in host and engineered tissues. *Acta Biomaterialia, 69*, 42-62. doi: 10.1016/j.actbio.2018.01.017.

Katyal, P., Mahmoudinobar, F., & Montclare, J. K. (2020). Recent trends in peptide and protein-based hydrogels. *Current Opinion in Structural Biology, 63*, 97-105. doi: 10.1016/j.sbi.2020.04.007.

Khanmohammadi, M., Dastjerdi, M. B., Ai, A., Ahmadi, A., Godarzi, A., Rahimi, A., & Ai, J. (2018). Horseradish peroxidase-catalyzed hydrogelation for biomedical applications. *Biomaterials Science, 6*(6), 1286-1298. doi: 10.1039/c8bm00056e.

Kim, C. S., Choi, Y. S., Ko, W., Seo, J. H., Lee, J., & Cha, H. J. (2011). A mussel adhesive protein fused with the BC domain of protein A is a functional linker material that efficiently immobilizes antibodies onto diverse surfaces. *Advanced Functional Materials, 21*(21), 4101–4108. doi: 10.1002/adfm.201100710.

Kim, J. J., Hou, L., & Huang, N. F. (2016). Vascularization of three-dimensional engineered tissues for regenerative medicine applications. *Acta Biomaterialia, 41*, 17-26. doi: 10.1016/j.actbio.2016.06.001.

Kim, S. Y., Wong, A. H., Abou Neel, E. A., Chrzanowski, W., & Chan, H. (2014). The future perspectives of natural materials for pulmonary drug delivery and lung tissue engineering. *Expert Opinion on Drug Delivery, 12*(6), 869-887. doi: 10.1517/17425247.2015.993314.

Kim, Y., Gill, W. W., & Liu, J. C. (2016). Enzymatic cross-linking of Resilin-based proteins for vascular tissue engineering applications. *Biomacromolecules, 17*(8), 2530−2539. doi: 10.1021/acs.biomac.6b00500.

King, W. J., & Krebsbach, P. H. (2012). Growth factor delivery: how surface interactions modulate release in vitro and in vivo. *Advanced Drug Delivery Reviews, 64*(12), 1239-1256. doi: 10.1016/j.addr.2012.03.004.

Kobayashi, K., Sato, K., Kida, T., Omori, K., Hori, M., Ozaki, H., & Murata, T. (2014). Stromal cell-derived factor-1α/C-X-C chemokine receptor type 4 axis promotes endothelial cell barrier integrity via phosphoinositide 3-kinase and Rac1 activation. *Arteriosclerosis, Thrombosis, and Vascular Biology, 34*(8), 1716-1722. doi: 10.1161/ATVBAHA.114.303890.

Korn, M. J., & Cramer, K. S. (2007). Windowing chicken eggs for developmental studies. *Journal of Visualized Experiments, 8*, 306. doi: 10.3791/306.

Kowalczyk, T., Hnatuszko-Konka, K., Gerszberg, A., & Kononowicz, A. K. (2014). Elastin-like polypeptides as a promising family of genetically-engineered protein based polymers. *World Journal of Microbiology & Biotechnology, 30*(8), 2141–2152. doi: 10.1007/s11274-014-1649-5.

Krishna, O. D., Jha, A. K., Jia, X., & Kiick, K. L. (2011). Integrin-mediated adhesion and proliferation of human MSCs elicited by a hydroxyproline-lacking, collagen-like peptide. *Biomaterials, 32*(27), 6412–6424. doi: 10.1016/j.biomaterials.2011.05.034.

Kuttappan, S., Mathew, D., Jo, J. I., Tanaka, R., Menon, D., Ishimoto, T., . . . Tabata, Y. (2018). Dual release of growth factor from nanocomposite fibrous scaffold promotes vascularisation and bone regeneration in rat critical sized calvarial defect. *Acta Biomaterialia, 78,* 36-47. doi: 10.1016/j.actbio.2018.07.050.

Lamalice, L., Boeuf, F. L., & Huot, J. (2007). Endothelial Cell Migration During Angiogenesis. *Circulation Research, 100*(6), 782-794. doi: 10.1161/01.RES.0000259593.07661.1e.

Lee, P. F., Yeh, A. T., & Bayless, K. J. (2009). Nonlinear optical microscopy reveals invading endothelial cells anisotropically alter three-dimensional collagen matrices. *Experimental Cell Research, 315*(3), 396-410. doi: 10.1016/j.yexcr.2008.10.040.

Lei, J., Sun, L., Huang, S., Zhu, C., Li, P., He, J., . . . He, Q. (2019). The antimicrobial peptides and their potential clinical applications. *American Journal of Translational Research, 11*(7), 3919-3931.

Leslie-Barbick, J. E., Shen, C., Chen, C., & West, J. L. (2011). Micron-scale spatially patterned, covalently immobilized vascular endothelial growth factor on hydrogels accelerates endothelial tubulogenesis and increases cellular angiogenic responses. *Tissue Engineering. Part A, 17*(1-2), 221-229. doi: 10.1089/ten.TEA.2010.0202.

Levenberg, S., Rouwkema, J., Macdonald, M., Garfein, E. S., Kohane, D. S., Darland, D. C., . . . Langer, R. (2005). Engineering vascularized skeletal

muscle tissue. *Nature Biotechnology, 23*(7), 879-884. doi: 10.1038/nbt1109.

Li, B., & Xiu, R. (2013). Angiogenesis: from molecular mechanisms to translational implications. *Clinical Hemorheology and Microcirculation, 54*(4), 345-355. doi: 10.3233/CH-121647.

Li, H., Yan, M., Yu, J., Xu, Q., Xia, X., Liao, J., & Zheng, W. (2020). In vivo identification of arteries and veins using two-photon excitation elastin autofluorescence. *Journal of Anatomy, 236*(1), 171-179. doi: 10.1111/joa.13080.

Li, L., Mahara, A., Tong, Z., Levenson, E. A., McGann, C. L., Jia, X., . . . Kiick, K. L. (2016). Recombinant resilin-based bioelastomers for regenerative medicine applications. *Advanced Healthcare Materials, 5*(2), 266–275. doi: 10.1002/adhm.201500411.

Li, L., Teller, S., Clifton, R. J., Jia, X., & Kiick, K. L. (2011). Tunable mechanical stability and deformation response of a resilin-based elastomer. *Biomacromolecules, 12*(6), 2302–2310. doi: 10.1021/bm200373p.

Li, M., Pathak, R. R., Lopez-Rivera, E., Friedman, S. L., Aguirre-Ghiso, J. A., & Sikora, A. G. (2015). The In Ovo Chick Chorioallantoic Membrane (CAM) Assay as an Efficient Xenograft Model of Hepatocellular Carcinoma. *Journal of Visualized Experiments, 104*, 52411. doi:10.3791/52411.

Li, R., Li, D. H., Zhang, H. Y., Wang, J., Li, X. K., & Xiao, J. (2020). Growth factors-based therapeutic strategies and their underlying signaling mechanisms for peripheral nerve regeneration. *Acta Pharmacologica Sinica, 41*(10), 1289-1300. doi: 10.1038/s41.

Luginbuhl, K. M., Mozhdehi, D., Dzuricky, M., Yousefpour, P., Huang, F. C., Mayne, N. R., . . . Chilkoti, A. (2017). Recombinant synthesis of hybrid lipid–peptide polymer fusions that self-assemble and encapsulate hydrophobic drugs. *Angewandte Chemie (International ed. in English), 56*(45), 13979–13984. doi: 10.1002/anie.201704625.

Lyons, R. E., Nairn, K. M., Huson, M. G., Kim, M., Dumsday, G., & Elvin, C. M. (2009). Comparisons of recombinant resilin-like proteins: Repetitive domains are sufficient to confer resilin-like properties. *Biomacromolecules, 10*(11), 3009-3014. doi: 10.1021/bm900601h.

Mackenzie, D. (1973). The history of sutures. *Medical History, 17*(2), 158–168. doi: 10.1017/s0025727300018469.

Maier, T., Leibundgut, M., & Ban, N. (2008). The crystal structure of a mammalian fatty acid synthase. *Science, 321*(5894), 1315-1322. doi: 10.1126/science.1161269.

Marshall, K. M., Kanczler, J. M., & Oreffo, R. O. (2020). Evolving applications of the egg: chorioallantoic membrane assay and ex vivo organotypic culture of materials for bone tissue engineering. *Journal of Tissue Engineering, 11*, 2041731420942734. doi: 10.1177/2041731420942734.

Masters, K. S. (2011). Covalent growth factor immobilization strategies for tissue repair and regeneration. *Macromolecular Bioscience, 11*(9), 1149-1163. doi: 10.1002/mabi.201000505.

Mastrullo, V., Cathery, W., Velliou, E., Madeddu, P., & Campagnolo, P. (2020). Angiogenesis in Tissue Engineering: As Nature Intended? *Frontiers in Bioengineering and Biotechnology , 8*, 188. doi: 10.3389/fbioe.2020.00188.

McGann, C. L., Levenson, E. A., & Kiick, K. L. (2013). Resilin-based hybrid hydrogels for cardiovascular tissue engineering. *Macromolecules, 214*(2), 203–213. doi: 10.1002/macp.201200412.

Mendes, G. G., Booth, R. M., Pattison, D. L., Alvarez, A. J., & Bondos, S. E. (2018). Generating Novel Materials Using the Intrinsically Disordered Protein Ubx. *Methods in Enzymology, 611*, 583-605. doi: 10.1016/bs.mie.2018.08.007.

Mitchell, A. C., Briquez, P. S., Hubbell, J. A., & Cochran, J. R. (2016). Engineering growth factors for regenerative medicine applications. *Acta Biomaterialia, 30*, 1-12. doi: 10.1016/j.actbio.2015.11.007.

Mitsos, S., Katsanos, K., Koletsis, E., Kagadis, G. C., Anastasiou, N., Diamantopoulos, A., . . . Dougenis, D. (2012). Therapeutic angiogenesis for myocardial ischemia revisited: basic biological concepts and focus on latest clinical trials. *Angiogenesis, 15*(1), 1-22. doi: 10.1007/s10456-011-9240-2.

Moreno-Jiménez, I., Kanczler, J. M., Hulsart-Billstrom, G., Inglis, S., & Oreffo, R. (2017). The Chorioallantoic Membrane Assay for Biomaterial Testing in Tissue Engineering: A Short-Term In Vivo Preclinical Model. *Tissue engineering. Part C, Methods, 23*(12), 938-952. doi: 10.1089/ten.tec.2017.0186.

Muffly, T. M., Tizzano, A. P., & Walters, M. D. (2011). The history and evolution of sutures in pelvic surgery. *Journal of the Royal Society of Medicine, 104*(3), 107-112. doi:10.1258/jrsm.2010.100243.

Nazeer, M. A., Karaoglu, I. C., Ozer, O., Albayrak, C., & Kizilel, S. (2021). Neovascularization of engineered tissues for clinical translation: Where we are, where we should be? *APL Bioengineering, 5*(2), 021503. doi: 10.1063/5.0044027.

Ngo, M., & Harley, B. A. (2020). Angiogenic biomaterials to promote therapeutic regeneration and investigate disease progression. *Biomaterials, 255*, 120207. doi: 10.1016/j.biomaterials.2020.120207.

Niu, Y., Li, Q., Ding, Y., Dong, L., & Wang, C. (2019). Engineered delivery strategies for enhanced control of growth factor activities in wound healing. *Advanced Drug Delivery Reviews, 146*, 190-208. doi: 10.1016/j.addr.2018.06.002.

Norooznezhad, A. H., Keshavarz, M., Norooznezhad, F., & Mansouri, K. (2017). Inhibition of Angiogenesis: A Novel Effect of Zataria Multiflora.

International Journal of Hematology-Oncology and Stem Cell Research, 11(2), 96-101.

Novosel, E. C., Kleinhans, C., & Kluger, P. J. (2011). Vascularization is the key challenge in tissue engineering. *Advanced Drug Delivery Reviews, 63*, 300-311. doi: 10.1016/j.addr.2011.03.004.

Nowak-Sliwinska, P., Segura, T., & Iruela-Arispe, M. L. (2014). The chicken chorioallantoic membrane model in biology, medicine and bioengineering. *Angiogenesis, 17*(4), 779-804. doi: 10.1007/s10456-014-9440-7.

Nurkesh, A., Jaguparov, A., Jimi, S., & Saparov, A. (2020). Recent Advances in the Controlled Release of Growth Factors and Cytokines for Improving Cutaneous Wound Healing. *Frontiers in Cell and Developmental Biology, 8*, 638. doi: 10.3389/fcell.2020.00638.

Park, J. S., Ahn, J. Y., Lee, S. H., Lee, H., Han, K. Y., Seo, H. S., . . . Lee, J. (2007). Enhanced stability of heterologous proteins by supramolecular self-assembly. *Applied Microbiology and Biotechnology, 75*(2), 347-355. doi: 10.1007/s00253-006-0826-3.

Park, S. H., Gil, E. S., Shi, H., Kim, H. J., Lee, K., & Kaplan, D. L. (2010). Relationships between degradability of silk scaffolds and osteogenesis. *Biomaterials, 31*(24), 6162-6172. doi: 10.1016/j.biomaterials.2010.04.028.

Parker, R. N., Cairns, D. M., Wu, W. A., Jordan, K., Guo, C., Huang, W., . . . Kaplan, D. L. (2020). Smart material hydrogel transfer devices fabricated

with stimuli-responsive silk-elastin-like proteins. *Advanced Healthcare Materials*, *9*(11), e2000266. doi: 10.1002/adhm.202000266.

Patterson, J. L., Abbey, C. A., Bayless, K. J., & Bondos, S. E. (2014). Materials composed of the Drosophila melanogaster protein Ultrabithorax are cytocompatible. *Journal of Biomedical Materials Research. Part A, 102*(1), 97-104. doi: 10.1002/jbm.a.34675.

Patterson, J. L., Arenas-Gamboa, A. M., Wang, T. Y., Hsiao, H. C., Howell, D. W., Pellois, J. P., . . . Bondos, S. E. (2015). Materials composed of the Drosophila Hox protein Ultrabithorax are biocompatible and nonimmunogenic. *Journal of Biomedical Materials Research. Part A, 103*(4), 1546-1553. doi: 10.1002/jbm.a.35295.

Pereira, A. M., Machado, R., da Costa, A., Ribeiro, A., Collins, T., Gomes, A. C., . . . Casal, M. (2017). Silk-based biomaterials functionalized with fibronectin type II promotes cell adhesion. *Acta Biomaterialia*, *47*, 50-59. doi: 10.1016/j.actbio.2016.10.002.

Petrou, G., Jansson, R., Högqvist, M., Erlandsson, J., Wågberg, L., Hedhammar, M., & Crouzier, T. (2018). Genetically engineered mucoadhesive spider silk. *Biomacromolecules, 19*(8), 3268-3279. doi: 10.1021/acs.biomac.8b00578.

Petzold, J., Aigner, T. B., Touska, F., Zimmermann, K., Scheibel, T., & Engel, F. X. (2017). Surface features of recombinant spider silk protein eADF4(k16)-made materials are well-suited for cardiac tissue engineering.

Advanced Functional Materials, 27(36), 1701427. doi: 10.1002/adfm.201701427.

Plowright, R., Dinjaski, N., Zhou, S., Belton, D. J., Kaplan, D. L., & Perry, C. C. (2016). Influence of silk-silica fusion protein design on silica condensation in vitro and cellular calcification. *RSC Advances, 6*(26), 21776-21788. doi: 10.1039/C6RA03706B.

Pritchard, E. M., & Kaplan, D. L. (2011). Silk fibroin biomaterials for controlled release drug delivery. *Expert Opinion on Drug Delivery, 8*(6), 797-811. doi: 10.1517/17425247.2011.56893.

Qiu, W., Teng, W., Cappello, J., & Wu, X. (2009). Wet-spinning of recombinant silk-elastin-like protein polymer fibers with high tensile strength and high deformability. *Biomacromolecules, 10*(3), 602-608. doi: 10.1021/bm801296r.

Ren, X., Zhao, M., Lash, B., Martino, M. M., & Julier, Z. (2020). Growth Factor Engineering Strategies for Regenerative Medicine Applications. *Frontiers in Bioengineering and Biotechnology, 7*, 469. doi: 10.3389/fbioe.2019.00469.

Renier, N., Wu, Z., Simon, D. J., Yang, J., Ariel, P., & Tessier-Lavigne, M. (2014). iDISCO: a simple, rapid method to immunolabel large tissue samples for volume imaging. *Cell, 159*, 896-910. doi: 10.1016/j.cell.2014.10.010.

Ribatti, D. (2012). Chicken chorioallantoic membrane angiogenesis model. *Methods in Molecular Biology, 843,* 47-57. doi: 10.1007/978-1-61779-523-7_5.

Ribatti, D. (2014). The chick embryo chorioallantoic membrane as a model for tumor biology. *Experimental Cell Research, 328*(2), 314-324. doi: 10.1016/j.yexcr.2014.06.010.

Ribatti, D., Gualandris, A., Bastaki, M., Vacca, A., Iurlaro, M., Roncali, L., & Presta, M. (1997). New model for the study of angiogenesis and antiangiogenesis in the chick embryo chorioallantoic membrane: the gelatin sponge/chorioallantoic membrane assay. *Journal of Vascular Research, 34*(6), 455-463. doi: 10.1159/000159256.

Ribatti, D., Vacca, A., Roncali, L., & Dammacco, F. (1996). The chick embryo chorioallantoic membrane as a model for in vivo research on angiogenesis. *The International Journal of Developmental Biology, 40*(6), 1189-1197.

Richardson, T. P., Peters, M. C., Ennett, A. B., & Mooney, D. J. (2001). Polymeric system for dual growth factor delivery. *Nature Biotechnology, 19,* 1029-1034. doi: 10.1038/nbt1101-1029.

Romano, N. H., Sengupta, D., Chung, C., & Heilshorn, S. C. (2011). Protein-engineered biomaterials: Nanoscale mimics of the extracellular matrix. *Biochimica et Biophysica Acta, 1810*(3), 339-349. doi: 10.1016/j.bbagen.2010.07.005.

Rouger, V., Alchini, R., Kazarine, A., Gopal, A. A., Girouard, M. P., Fournier, A. E., & Wiseman, P. W. (2016). Low-cost multimodal light sheet microscopy for optically cleared tissues and living specimens. *Journal of Biomedical Optics, 21*, 126008. doi: 10.1117/1.JBO.21.12.126008.

Rous, P., & Murphy, J. B. (1911). Tumor implantations in the developing embryo. *The Journal of the American Medical Association, 10*(56), 741-742. doi:10.1001/jama.1911.02560100033015.

Rouwkema, J., & Khademhosseini, A. (2016). Vascularization and Angiogenesis in Tissue Engineering: Beyond Creating Static Networks. *Trends in Biotechnology, 34*(9), 733-745. doi: 10.1016/j.tibtech.2016.03.002.

Rouwkema, J., Rivron, N. C., & van Blitterswijk, C. A. (2008). Vascularization in tissue engineering. *Trends in Biotechnology, 26*(8), 434-441. doi: 10.1016/j.tibtech.2008.04.009.

Salcedo, R., Wasserman, K., Young, H., Grimm, M., Howard, O., Anver, M., & et al. (1999). Vascular endothelial growth factor and basic fibroblast growth factor induce expression of CXCR4 on human endothelial cells: In vivo neovascularization induced by stromal-derived factor-1alpha. *The American Journal of Pathology, 154*(4), 1125-1135. doi: 10.1016/s0002-9440(10)65365-5.

Sawle, L., & Ghosh, K. (2011). How do thermophilic proteins and proteomes withstand high temperature? *Biophysical Journal, 101*(1), 217-227. doi: 10.1016/j.bpj.2011.05.059.

Seliktar, D. (2012). Designing cell-compatible hydrogels for biomedical applications. *Science, 336*(6085), 1124-1128. doi: 10.1126/science.1214804.

Sharon, J., & Puleo, D. (2008). Immobilization of glycoproteins, such as VEGF, on biodegradable substrates. *Acta Biomaterialia, 4*(4), 1016-1023. doi: 10.1016/j.actbio.2008.02.017.

Silva, N. H., Vilela, C., Marrucho, I. M., Freire, C. S., Pascoal Neto, C., & Silvestre, A. J. (2014). Protein-based materials: from sources to innovative sustainable materials for biomedical applications. *Journal of Materials Chemistry. B, 2*, 3715-3740. doi: 10.1039/c4tb00168k.

Silva, R., Fabry, B., & Boccaccini, A. R. (2014). Fibrous protein-based hydrogels for cell encapsulation. *Biomaterials, 35*(25), 6727-6738. doi: 10.1016/j.biomaterials.2014.04.078.

Simons, M., & Ware, J. (2003). Therapeutic angiogenesis in cardiovascular disease. *Nature Reviews Drug Discovery, 2*(11), 863-871. doi: 10.1038/nrd1226.

Solomonov, A., & Shimanovich, U. (2019). Self-assembly in protein-based bionanomaterials. *Israel Journal of Chemistry, 60*(12), 1152-1170. doi: 10.1002/ijch.201900083.

Song, H. G., Rumma, R. T., Ozaki, C. K., Edelman, E. R., & Chen, C. S. (2018). Vascular Tissue Engineering: Progress, Challenges, and Clinical Promise. *Cell Stem Cell, 22*(3), 340-354. doi: 10.1016/j.stem.2018.02.009.

Taniguchi, M., Saito, K., Aida, R., Ochiai, A., Saitoh, E., & Tanaka, T. (2019). Wound healing activity and mechanism of action of antimicrobial and lipopolysaccharide-neutralizing peptides from enzymatic hydrolysates of rice bran proteins. *Journal of Bioscience and Bioengineering, 128*(2), 142-148. doi: 10.1016/j.jbiosc.2019.02.002.

Taniguchi, Y. (2017). Autofluorescence imaging of tissue samples using super-high sensitivity fluorescence microscopy. *Global Imaging Insights, 2*, 1-2. doi: 10.15761/GII.1000135.

Thatikonda, N., Delfani, P., Jansson, R., Petersson, L., Lindberg, D., Wingren, C., & Hedhammar, M. (2016). Genetic fusion of single-chain variable fragments to partial spider silk improves target detection in micro- and nanoarrays. *Biotechnology Journal, 11*(3), 437-448. doi: 10.1002/biot.201500297.

Thatikonda, N., Nilebäck, L., Kempe, A., Widhe, M., & Hedhammar, M. (2018). Bioactivation of Spider Silk with Basic Fibroblast Growth Factor for in Vitro Cell Culture: A Step toward Creation of Artificial ECM. *ACS Biomaterials Science and Engineering, 4*, 3384-3396. doi: 10.1021/acsbiomaterials.8b00844.

Tsai, S. P., Howell, D. W., Huang, Z., Hsiao, H. C., Lu, Y., Matthews, K. S., . . . Bondos, S. E. (2015). The Effect of Protein Fusions on the Production and Mechanical Properties of Protein-Based Materials. *Advanced Functional Materials, 25*, 1442-1450. doi: 10.1002/adfm.201402997.

U.S. Food and Drug Administration. (2008). *Safety Warning on Becaplermin in Regranex.* Silver Spring: MD.

Ucuzian, A., Gassman, A. A., East, A., & Greisler, H. (2010). Molecular mediators of angiogenesis. *Journal of Burn Care & Research, 31*(1), 158-175. doi: 10.1097/BCR.0b013e3181c7ed82.

Unzueta, U., Seras-Franzoso, J., Céspedes, M. V., Saccardo, P., Cortés, F., Rueda, F., . . . Villaverde, A. (2017). Engineering tumor cell targeting in nanoscale amyloidal materials. *Nanotechnology, 28*(1), 015102. doi: 10.1088/0957-4484/28/1/015102.

Urello, M. A., Kiick, K. L., & Sullivan, M. O. (2014). A CMP-based method for tunable, cell-mediated gene delivery from collagen scaffolds. *Journal of Materials Chemistry B, 2*(46), 8174-8185. doi: 10.1039/C4TB01435A.

Vashist, S. K., Marion Schneider, E., Lam, E., Hrapovic, S., & Luong, J. H. (2014). One-step antibody immobilization-based rapid and highly-sensitive sandwich ELISA procedure for potential in vitro diagnostics. *Scientific Reports, 4*, 4407. doi: 10.1038/srep04407.

Vornholt, T., & Jeschek, M. (2020). The Quest for Xenobiotic Enzymes: From New Enzymes for Chemistry to a Novel Chemistry of Life. *ChemBioChem, 21*(16), 2241-2249. doi: 10.1002/cbic.202000121.

Włodarczyk-Biegun, M. K., Werten, M. W., de Wolf, F. A., van den Beucken, J. J., Leeuwenburgh, S. C., Kamperman, M., & Cohen Stuart, M. A. (2014). Genetically engineered silk-collagen-like copolymer for biomedical

applications: production, characterization and evaluation of cellular response. *Acta Biomaterialia, 10*(8), 3620-3629. doi: 10.1016/j.actbio.2014.05.006.

Wang, X., Ali, M. S., & Lacerda, C. M. (2018). Three-dimensional collagen-elastin scaffold for heart valve tissue engineering. *Bioengineering (Basel), 5*(3), 69. doi: 10.3390/bioengineering5030069.

Wang, Y., Rudym, D. D., Walsh, A., Abrahamsen, L., Kim, H. J., Kim, H. S., . . . Kaplan, D. L. (2008). In vivo degradation of three-dimensional silk fibroin scaffolds. *Biomaterials, 29*(24-25), 3415-3428. doi: 10.1016/j.biomaterials.2008.05.002.

Wang, Z., Kluge, J. A., Leisk, G. G., & Kaplan, D. L. (2008). Sonication-induced gelation of silk fibroin for cell encapsulation. *Biomaterials, 29*(8), 1054-1064. doi: 10.1016/j.biomaterials.2007.11.003.

Wang, Z., Wang, Z., Lu, W. W., Zhen, W., Yang, D., & Peng, S. (2017). Novel biomaterial strategies for controlled growth factor delivery for biomedical applications. *NPG Asia Materials, 9*, e435. doi: 10.1038/am.2017.171.

Ware, J., & Simons, M. (1997). Angiogenesis in ischemic heart disease. *Nature Medicine, 3*(2), 158-164. doi: 10.1038/nm0297-158.

Wei, G., Su, Z., Reynolds, N. P., Arosio, P., Hamley, I. W., Gazit, E., & Mezzenga, R. (2017). Self-assembling peptide and protein amyloids: from structure to tailored function in nanotechnology. *Chemical Society Reviews, 46*(15), 4661-4708. doi: 10.1039/c6cs00542j.

Whittington, N. C., & Wray, S. (2017). Suppression of Red Blood Cell Autofluorescence for Immunocytochemistry on Fixed Embryonic Mouse Tissue. *Current Protocols in Neuroscience, 81*, 2.28.1-2.28.12. doi: 10.1002/cpns.35.

Widhe, M., Shalaly, N. D., & Hedhammar, M. (2016). A fibronectin mimetic motif improves integrin mediated cell biding to recombinant spider silk matrices. *Biomaterials, 74*, 256-266. doi: 10.1016/j.biomaterials.2015.10.013.

Witsch, E., Sela, M., & Yarden, Y. (2010). Roles for growth factors in cancer progression. *Physiology (Bethesda), 25*(2), 85-101. doi: 10.1152/physiol.00045.2009.

Wolinsky, J. B., Colson, Y. L., & Grinstaff, M. W. (2012). Local drug delivery strategies for cancer treatment: Gels, nanoparticles, polymeric films, rods, and wafers. *Journal of Controlled Release, 159*(1), 14-26. doi: 10.1016/j.jconrel.2011.11.031.

Xu, H. L., Yu, W. Z., Lu, C. T., Li, X. K., & Zhao, Y. Z. (2017). Delivery of growth factor-based therapeutics in vascular diseases: Challenges and strategies. *Biotechnology Journal, 12*, 1600243. doi: 10.1002/biot.201600243.

Yang, G., Mahadik, B., Choi, J. Y., & Fisher, J. P. (2020). Vascularization in tissue engineering: fundamentals and state-of-art. *Progress in Biomedical Engineering, 2*, 012002. doi: 10.1088/2516-1091/ab5637.

Yao, T., Baker, M., & Moroni, L. (2020). Strategies to Improve Nanofibrous Scaffolds for Vascular Tissue Engineering. *Nanomaterials (Basel), 10*(5), 887. doi: 10.3390/nano10050887.

Yeo, G. C., Aghaei-Ghareh-Bolagh, B., Brackenreg, E. P., Hiob, M. A., Lee, P., & Weiss, A. S. (2015). Fabricated Elastin. *Advanced Healthcare Materials, 4*(16), 2530-2556. doi: 10.1002/adhm.201400781.

Zachary, I. (2003). Integration of Mitogenic and Migratory Signals from G-Protein-Coupled Receptors and Tyrosine Kinases. *Biochemical Society Transactions, 31*, 1171-1177. doi: 10.1042/bst0311171.

Zhang, R., Zhang, Y., & Yi, S. (2019). Identification of critical growth factors for peripheral nerve regeneration. *RSC Advances, 9*, 10760-10765. doi: 10.1039/C9RA01710K.

Zhou, J., Cao, C., Ma, X., Hu, L., Chen, L., & Wang, C. (2010). In vitro and in vivo degradation behavior of aqueous-derived electrospun silk fibroin scaffolds. *Polymer Degradation and Stability, 95*(9), 1679-1685. doi: 10.1016/j.polymdegradstab.2010.05.025.

Zhou, X. M., Entwistle, A., Zhang, H., Jackson, A. P., Mason, T. O., Shimanovich, U., . . . Perrett, S. (2014). Self-assembly of amyloid fibrils that display active enzymes. *ChemCatChem, 6*(7), 1961-1968. doi: 10.1002/cctc.201402125.

Zhu, X., & Xiong, L. (2013). Putative megaenyme DWA1 plays essential roles in drought resistance by regulating stress-induced wax deposition in rice.

Proceedings of the National Academy of Sciences of the United States of America, *110*(44), 17790-17785. doi: 10.1073/pnas.1316412110.